SINTERING OF SUBMICRON WC BASED HARD METALS

by

SUBIR KUMAR BHAUMIK

DEPARTMENT OF METALLURGICAL ENGINEERING

INDIAN INSTITUTE OF TECHNOLOGY, KANPUR

APRIL, 1986

SINTERING OF SUBMICRON WC BASED HARD METALS

A Thesis Submitted
in Partial Fulfilment of the Requirements
for the Degree of

MASTER OF TECHNOLOGY

by

SUBIR KUMAR BHAUMIK

to the

DEPARTMENT OF METALLURGICAL ENGINEERING
INDIAN INSTITUTE OF TECHNOLOGY, KANPUR
APRIL 1986

16/4/85

CERTIFICATE

This is to certify that the present work entitled "Sintering of Submicron WC Based Hard Metals" has been carried out by Mr. Subir Kumar Bhaumik under my supervision and it has not been submitted elsewhere for a degree.

15/4/85

G. S. UPADHYAYA
Professor
Department of Metallurgical Engineering
Indian Institute of Technology
Kanpur, India

ACKNOWLEDGEMENTS

The author, hereby takes the privilege to tender his deepest reverence and heartiest indebtedness to his thesis supervisor Prof. G.S. Upadhyaya for his earnest involvement, competent guidance and lively impetus without which it would not have been possible to complete this venture.

The author expresses his gratitude and deepest respect to Mr. N.M. Pai, Technical Director of 'Powder Metals and Alloys Pvt. Ltd.' for allowing his laboratory facilities to perform some of the experiments related to this thesis. Special thanks are due to M/s S.C. Soni, M.N. Mungole and B. Sharma for their everyday help during the course of this work.

The author expresses his thanks to all his friends particularly Mr. V. Shrikanth, S. Roy, R. Hulyal, S.V.V. Ramana and P.P. Mukherjee for their co-operation and moral support during the course of this work.

Last but not the least, M/s R.N. Srivastava and B.K. Jain are to be acknowledged gratefully for excellent typing and tracing work respectively.

- Subir Kumar Bhaumik

TABLE OF CONTENTS

ABSTRACT

The present investigation covers the sintering studies of submicron WC based hardmetals containing 10% Co. Cobalt was substituted either partially or completely by Ni, Fe or Ni/Fe. Milling was done for 24 hours and sintering at 1350°C and 1400°C in dry H_2 for 1 hour respectively. The results show better sintered properties in WC-10(Ni/Fe) hardmetals. Grain growth took place when Co was substituted by Ni or Fe or Ni/Fe. Oxidation of WC-10(Co/Ni) hardmetals were carried out at 800°C for 8 hours in air to have an idea on the variation in binder composition on the oxidation resistance. The results revealed that Ni addition decreases the oxidation resistance of WC-10 Co hardmetal. Refractory compounds like TiC, TiC-Mo_2C, TiN and TiB_2 were also added to study their effects on the properties of WC-10 Co hardmetal. Out of these TiB_2 addition showed the poorest effect. Ni_2P was also added to the WC-10(Co/Ni) hardmetals to lower the sintering temperature but the end properties were not promising ones.

CHAPTER - I

LITERATURE REVIEW

I.1 Introduction:

Conventional WC is mainly manufactured with cobalt as binder phase. Cobalt is choosen as the binder in cemented carbides due to its good wetting behaviour, temperature dependent solubility and good mechanical properties.[1] But due to its high cost and limited resources efforts have been made to replace cobalt by other iron group metals.

According to Tracy and Hall[2] cobalt can be totally replaced by nickel upto 6% binder without sacrificing the hardness value, but further increase in nickel content in the binder decreases the hardness sharply. They found that sintering temperature of Ni bonded hard metal is 50-75°C greater than that of Co bonded one and its introduction to WC gives rise to detrimental free carbon in the system. But the partial substitution of Co by Ni reduces the sintering temperature by about 30°C as in the ternary system the eutectic liquid forms at 1300°C. Schwarzkopf and Kieffer[3] found that hard metals bonded with iron or nickel do not show more than 40-60% of the transverse rupture strength as to that of cobalt bonded tungsten carbides.

If similar procedures as that of Co bonded cemented carbides are employed in the preparation of Fe bonded tungsten carbides so that WC of theoretical carbon content is bonded with Fe, it is found that the double carbide Fe_3W_3C forms.

This explains the lack of success in attempts to replace Co with Fe. Although sintered tungsten carbide-iron alloys are notable for their lack of commercial utilization, it has been reported[4] that additions of free carbon to Fe-WC alloys exceeding the stoichiometric amount required for the tungsten carbide can inhibit the formation of large grains of the brittle 'eta' phase. Agte[5] successfully replaced cobalt through iron-nickel alloy by using tungsten carbide with a carbon content that was hyperstoichiometric. A. Suzuki and co-workers[6,7] studied the influence of carbon content on the properties of WC-Fe and WC-Fe/Ni cemented carbides and found that these alloys were inferior to WC-Co. However, Moskowitz and co-workers[8,9] came to quite the opposite conclusion. They have shown that the Fe:Ni ratio and C-content are the property determining factors for WC-Fe/Ni alloys. Hora[10] has also shown that WC alloys cemented with an iron rich Fe/Co/Ni alloy posses good properties. However cobalt rich Fe/Co/Ni binder alloys lead to cemented carbides with inferior properties.[11]

Straight WC-Co hard metal is not universally applicable for all cutting applications, the role of refractory compounds additives is an important one. So from the practical point of view work is being going on to develop WC-based cemented carbides with refractory compounds addition to make a wide variation in the hardness properties of the hard metals.

Work on the improvement of WC-cemented carbides was carried out by improving on the binder phase of these hardmetals. This was tried by choosing Co-Ni, Co-Fe and Ni-Fe alloys as the

binder phase. And also experiment has been carried out with partial substitution of WC by refractory compounds like TiC, TiC-Mo_2C, TiB_2, TiN for wide wariation in the properties of WC-based hardmetals.

I.2 Sintering of WC-Co Cemented Carbides:

Pure WC can be sintered but it requires high temperature and such materials cannot be used in service condition which demands high hardness, abrassion resistance along with considerable strength. So generally Co is added with WC to lower the sintering temperature as well as to achieve the service required properties. Co is mostly used binder metal because this fulfills the following three conditions which is essential for compacts: (i) it supplies a liquid phase relatively at lower temperature, (ii) it is capable of dissolving WC and finally (iii) the liquid phase is able to wet the solid carbide particles completely.

From Figure 1.1 it is clear that the eutectic liquid forms in this system at 1320°C. Most commercially used hardmetal is 90 WC-10 Co and sintering is done at 1400°C. At 1400°C the liquid phase is about 15 wt % of the compact and the phases are WC and liquid phase i.e. WC dissolved in Co. Upon cooling the WC particles precipitates first and then the solidification is completed by eutectic reaction. In most cases, WC is precipitated on the surface of the undissolved carbide thus leading to grain growth. But recently it has been confirmed that formation of eutectic structure is not observed under

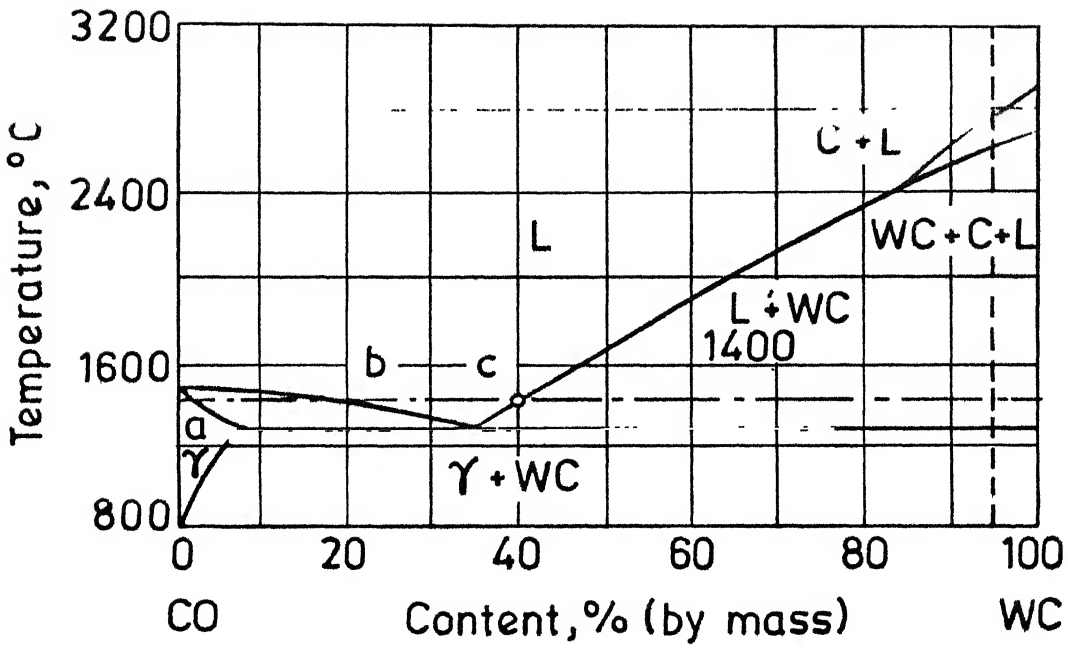

Fig. 1.1 Phase diagram for WC-Co system.

technical sintering conditions.[12] The η phase solidifies with about 20-25% WC in solid solution but the solubility decreases with decrease of temperature and in fact at room temperature the η phase contains less than 1.0% WC in solid solution.

The changes that is going on during sintering can be explained by Figure 1.2, which shows the shrinkage curve of typical WC-Co alloys with 6-12% Co and near stoichiometric carbon content. Many often it is said that densification of WC-Co alloys takes place in presence of liquid phase. Howsoever, appreciable shrinkage in the temperature interval between 800 and and 1250°C was noticed.[13] When the eutectic liquid is formed at 1280°C, a reduction of shrinkage rate takes place. This is due to the fact that the liquid penetrate the aggregate boundaries or grain boundaries and thus pushing the particle apart. But this is for very short interval. As the liquid phase penetrates the boundaries, substantial capilary force is developed which leads to the rearrangement of the particles in the liquid phase and ultimately complete densification is achieved. Further holding at maximum sintering temperature results in final modification in the microstructure i.e. the Co distribution, the carbide grain size, the grain shape and eventually the carbon content. It is interesting to note that the rate of shrinkage due to rearrangement in the solid and liquid stages seems to be controlled by same elementary factors. This is indicated by the facts that no discontinuity in shrinkage rate has been observed below and above the melting point which is also evident from Figure 1.2. So judging from the effective activation

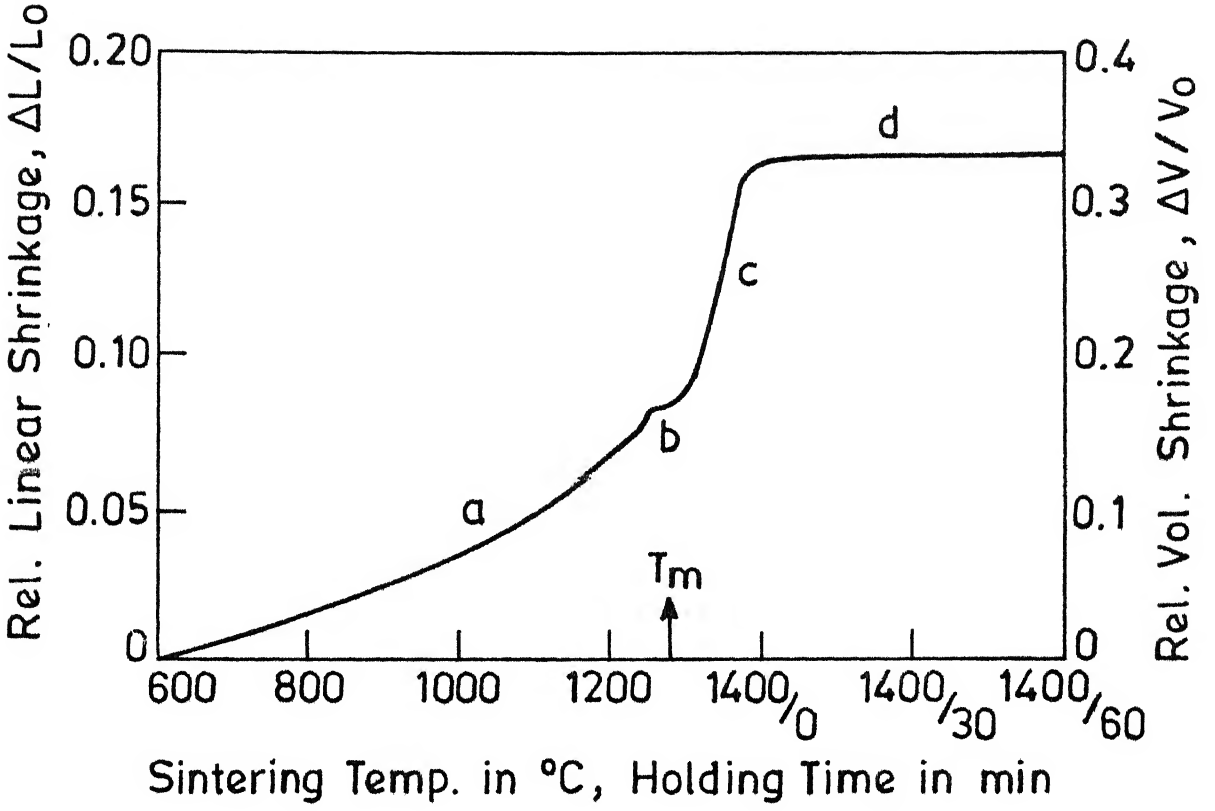

Fig. 1.2 Schematic shrinkage curve of std. WC-Co alloy. The melting temperature (T_m) and the main processes are indicated

a. Rearrangement in solid phase, adjustment of C content and Co distribution
b. Penetration of particle boundaries by liquid.
c. Rearrangement in liquid phase
d. Adjustment of microstructure and C content.

energy as well as from effect of carbon content on shrinkage rate, the solution of WC in Co plays a major role as the rate controlling factor. Even at rather low temperature Co spreads over the surfaces and/or penetrates the boundaries of WC crystals smoothing the surface. This effect facilitate gliding of WC particles providing mechanisms of rearrangement and denser packing.

Several other phenomena of practical importance occur in this presintering temperature range. The Co distribution becomes more uniform thus reducing the danger of forming Co pools. The carbon content is easily changed during this period because the furnace atmosphere is still in contact with the carbide. When shrinkage proceeds the carbon exchange between the atmosphere and the carbide crystals is retarded and equilibrium is not reached during the normal sintering periods. Thus the final carbon content of the alloy is essentially determined by the carbon content after presintering. During non-isothermal liquid phase sintering a high carbon content improves the cobalt distribution and results the earlier densification but also enhances the grain growth.

The mechanical properties of WC-Co hardmetal are known to depend on the carbon content. This question has been examined by Gurland[14] and in recent years particularly by Suzuki and co-workers.[15] According to Nishiyama and Ishida[16] the tungsten content of the binder depends upon the total carbon content. Therefore, some tests were carried out with WC-25 Co alloys sintered in same manner, but having different carbon

percentages. The chemical analysis of the isolates shows that the amount of tungsten in the isolates decreases as the carbon content of the specimen increases.

In most of the cases sintering is done in H_2 atmosphere. So during sintering the furnace atmosphere picks up some carbon from compacts to produce CH_4 and thereby loss of carbon takes place. To prevent this either equilibrium amount of CH_4 is passed with H_2 or additional amount of carbon is provided to encounter this loss. Sometimes to solve this problem sintering is done in vacuum. But there also problems arises. The vapour pressure of Co at sintering temperature is very high and if the temperature and pressure are not controlled carefully, excessive evaporation of Co may takes place from the external part of the sintered material. It is seen that below 10^{-2} Torr pressure, the evaporation rate is practically independent of pressure. So it is advisable to work under few Torrs, in order to reduce cobalt losses.(17)

Once a small amount of liquid is formed its further formation is rapid as surface tension forces result in rapid spreading and wetting of the surfaces of all other particles. At first the fine fraction of WC is most affected as the temperature is increased more carbide is dissolved. Possibly even before the steady temperature is reached there is continuous solution of fines and the corresponding deposition of carbide on already existing coarser carbide particles. Thus in the early stages of sintering fine particles rapidly disappear and the coarser tend to grow at the expense of finer particles.

Very fine carbide particles are extensively sensitive to this effects if the minimum sintering temperature exceeds. Thus, materials of mixed grain size, however, are more sensitive to grain growth because of the high surface energy of the finer grains. Uniform grain size products are particularly insensitive to sintering temperature and will show little change in grain size over a wide range of sintering conditions. As would be expected, the rate of grain growth increases rapidly with increasing temperature. At constant temperature grain growth will continue but only slowly. Thus sintering at a constant time and temperature will give a constant grain size in the finished product only if the initial powders were of the same average grain size and grain size distribution. Many additions can be made to hardmetals which will greatly restrict the rate of grain growth during sintering. Generally any such grain growth inhibitor also reduces the strength of the sintered products. So limited use is made to aid grain size control during sintering. The very fine grain products ($\leqslant 1$ µm) are those most prone to give grain growth trouble during sintering. These products are made for extreme wear and abrasive resistance. For such applications some strength can be sacrificed to achieve maximum wear resistance and it is not uncommon to use some grain growth inhibitors for such products. Among the grain growth inhibitors the most effective one is VC, which on 0.05% use can have a very useful effect on minimising grain size during sintering. Other additions that can be used are the carbides of Cr, Ta and Ti. But when high toughness along

with fine grain size is requires, we cannot use such grain growth inhibitor. In this case grain growth control has to be obtained by accurately controlled powder manufacture and careful controlled sintering conditions.(18)

Cobalt content also plays some part in the grain growth characteristics of hard metal during sintering. The 'heavy metal' grain growth mechanism is clearly dependent upon the amount of solvent metal phase available to allow transfer from fine to coarse particles. At cobalt contents above ~10% this is the dominant grain growth mechanism, but at lower cobalt contents, and especially with the carbides of finer grain size where carbide to carbide grain boundaries are more prevalent, another grain growth mechanism becomes evident. This can lead to exaggerated grain growth effects in which a few grains become highly coarser than the average. This effect is not observed with high cobalt alloys whe-e grain growth tends to produce a more uniform grain size as it becomes coarser. These effects are discussed in great detail by Exner and Fischmeister.(19)

I.3 Properties of WC-Co Cemented Carbides:

I.3.1 Sintered Density, Porosity

As the liquid phase sintering technique is essential in the processing of hard metals so almost close to theoretical density can be obtained. This property is very important as the sintering condition can be known by it. Moreover, other properties are also very much dependent on porosity.

Brooks[20] got the sintered density for 6%, 9% and 12% Co containing WC-Co hardmetals to be 15.02 gm/cc, 14.96 gm/cc and 14.67 gm/cc respectively. Ingelstrom and Nordberg[21] found that final sintered density varies with the particle size of Co and WC. They got the density of WC-Co (6%) to be 14.85 gm/cc when the particle size is medium. They studied with various Co content and various initial particle size and concluded that within the initial particle size of 1.0 to 3.3 m, the coarser the particle size, greater the sintered density.

I.3.2 Transverse Rupture Strength (T.R.S.)

Transverse rupture strength is an ultimate strength property which is used as a standard in the carbide industry. It is the calculated maximum tensile stress at failure of a carbide beam loaded midway between the supports. T.R.S. is a combination of shear strength, compressive strength and tensile strength.

Cemented carbides are intrinsically very strong but this strength is not realized in practice because of the inevitable presence of defects in the structure or at the surfaces at which stress concentrations arise when a stress is applied. These stress concentrations cannot be relieved by local plastic deformation so that the failure stress is reached at the points of stress concentration while the average applied stress is well below this level. Hence the failure load of a component made from a brittle material will depend upon the nature and distribution of the defects. In the same way, the failure load in transverse rupture test on cemented carbide is most

generally the load required to produce the fracture stress at some critical stress concentrating defect in the structure or on the tension surface of the test piece. Thus the fracture load is a function of both the intrinsic strength of the cemented carbide grade concerned and the nature and distribution of the defects within the structure. This has been studied in some detail in recent years. A number of co-workers[22-24] have shown that if broken transverse rupture test pieces of normal commercial quality cemented carbide are examined by modern fractographic methods the vast majority of the fractures can be shown to have initiated at internal defects in the material, not at the tensile surface of the test piece. These defects have been shown to be voids, inclusions, abnormally large WC grains, segregated areas or lakes of binder phase.

Engle[25] studied the variation of T.R.S. values of WC-Co hardmetals with Co content and suggests that T.R.S. at first increases with Co content then reaches a maximum at about 18% Co and substantially decreases.

Gurland[26] studied the influence of C in WC on the hardness and T.R.S. of an alloy with 16% Co and observed that strength curve passes through a maxima at a C content corresponding to stoichiometric carbon content of WC (6.12%). The strength decrease along carbon deficiency is much more pronounced than a carbon excess. Lardner[27] on an alloy with 8 wt % Co studied the relationship between the amount of phase and T.R.S. values and observed that T.R.S. values remain constant when the hardmetals contain between 0.5 vol % graphite and

0.5 vol % η phase and outside this range the value substantially decreases.

Rudiger and Exner[28] observed the effect of heat treatment on the T.R.S. properties of hardmetals. A hardening of Co through Co_3W is possible because of the strong temperature dependence of the solubility of W. They found that when the sample is heat treated at 1350°C the T.R.S. is appreciably improved.

I.3.3 Compressive Strength

The compressive strength of WC-Co is of great importance. In the complex form of loading to which hardmetals are subjected during the machining of metals and rock drilling, compression invariably plays a major part. Like T.R.S. compressive strength also passes through a maximum at a particular Co content depending on temperature and grain size. Compared to T.R.S. loading, however, the maximum for compressive loading occurs at a much lower Co content viz. at 6%.[29]

Kreimer et.al.[30] found that for each grain size the compressive strength passes through a maximum at a particular Co content, but the highest value is attained for fine grained hardmetals at 4% Co.

I.3.4 Tensile Strength

Very little has been published on the tensile strength of hardmetals because of experimental difficulties. According to Tretyakov[31] the tensile strength of the hardmetal with 6% Co is 73 Kg/mm^2 and that of hardmetal with 12% Co is 120 Kg/mm^2, while according to National Bureau of Standards in

America σ_t of the former hardmetal is 124 Kg/mm^2 and that of hardmetal of 13% Co is 143 Kg/mm^2. Recently it has been found out that like T.R.S. and compressive strength the plot of σ_t also passes through a maximum at 37% Co content. The tensile/transverse rupture strength ratio over the Co content of 65 to 10% Co found to vary between 0.56 and 0.46.

I.3.5 Fracture Toughness

Several scientists studied this property of the WC-Co hardmetals. Warren and Matzke[32] preferred Vickers diamond indentation and Hertzian indentation tests to investigate the fracture toughness. They claim that diamond indentation is a sensitive and reproducible method of toughness testing and the results can be empirically related to conventional toughness parameter. Nakamura and Gurland[33] tested this property by using single edge notched beam specimen and could not find any dependence of k_{IC} on temperature. They measured the fracture toughness of WC-Co two phase hardmetals as a function of WC grain size, mean free path of Co binder and/or volume fraction of WC grains using SENB specimen with a notch formed by Electron Discharge Machining (EDM).

I.3.6 Hardness

Hardness is one of the most important properties of hardmetals. Gurland and Bardzil[34] established the existence of a linear relationship between the hardness (Rockwell A) of WC-Co hardmetals and the logrithm of the mean distance, measured metallographically, between carbide grains. Kremier et.al.[30] investigated the effect of Co content and the mean carbide

grain size on the room temperature hardness of WC-Co hardmetals. Platov[35] in his study of the hardness of WC-Co hardmetals with various Co content and carbide grain sizes, demonstrated the validity of Meyer's law for WC-Co hardmetals and metallic Co

$$P = ad^n$$

where P is the load on the indentor, d is the impression diameter, a is the deformation resistance and n is a dimensionless parameter.

Lee and Gurland[36] also attempted to relate the hardness of cemented carbide with microstructure. They suggested that the carbide particles form a partially connected structure with long range continuity through direct carbide carbide contacts. The concept of plastic limit analysis is used to evaluate the effect of the continuous carbide phase on the hardness of WC-Co hardmetals and the following equation proposed.

$$H_C = H_{WC} \cdot V_{WC} \cdot C + H_m(1 - V_{WC} \cdot C)$$

while C is contiguity of the phase.

The hardness of carbide and matrix phases are the functions of particle size d, and binder mean free path λ respectively and are related by the empirical equation

$$H_{WC} = 1382 + 23.1\ d^{-1/2}\ (Kg/mm^2)$$

$$H_m = 304 + 12.7\ \lambda^{-1/2}\ (Kg/mm^2)$$

Altmeyer and Jung[37] claim that hardness does not vary linearly with temperature. They plotted the hardness of WC-Co hardmetals and pure Co against temperature in semilog co-ordinates and got two straight line sections with an inflection at a temperature range of 620-700°K for WC-Co. The relationship can be described by the following empirical formula

$$\ln H_T = \ln A - BT$$

The authors suggest that the inflection in the logrithm of hardness vs. temperature curve is linked with the recovery or recrystallisation of the Co phase and with the allotropic transition $Co^{(\varepsilon)}_{hex} - Co^{(\beta)}_{f.c.c.}$. Kalish and Gibbs[38] found that β phase and graphite content and grain size has similar effect on T.R.S. and hardness.

I.3.7 Wear Resistance

It has been seen that influence of Co content and carbide grain size on the wear resistance of the hardmetals is basically analogous to the influence of these parameters on their hardness. The wear resistance decreases with increasing Co content and grain size. Khrushehov and Babichev[39] established the relationship for pure metal

$$\varepsilon = - bH$$

where ε = magnitude of wear resistance, b = coefficient and H = hardness.

They measured the wear resistance of WC to be 2520 Kg/mm^2 while that of WC-6% Co to be 1950 Kg/mm^2 which shows that they follow this equation.

I.3.8 Oxidation Resistance

It has been noted that for oxidation of carbides, temperature in excess of 700°C is needed. Oxidation resistance of the hardmetals is very important property as at the cutting edges there is always high temperature and hence a fear of oxidation of the carbides.

Shan and Pandey[40] studied the oxidation behaviour of carbide cutting tools under the influence of an externally applied e.m.f. They found that for constant surface area of carbide tools, the weight of oxides formed under given conditions increased with increasing current through the cast iron-carbide tool interface. They also noticed that oxides are single phase compounds and their chemical composition and structure depend on the current passed through the interface.

I.3.9 Magnetic Properties

Coercivity is very important property by which we can get an idea about the distribution of Co binders within the system. Structure coarsening and decarburization can also be determined by coercive force. Sufficient data are available in the literature about the variation of coercivity values with composition, grain size etc.

Roebuck and Almond[41] along with many others observed that coercivity of the system decreases as the Co percentage increases and also when grain size increases.

Freytag and Exner[42] observed that magnetic saturation is sensitive to η phase formation not only if the system is a deficient but also when high carbon alloys quickly cooled from

sintering temperature. Therefore magnetic saturation is not a mere indication for the amount of W dissolved in the binder phase.

I.4 Substitution of Binder by Other Metals:

Co is used most extensively as the bonding metal with the WC based hardmetals. This is because of the very good solubility of WC in Co at the eutectic temperature which helps to form perfect bonding between the two dissimilar materials like WC and Co. Secondly at the eutectic temperature Co wets the WC grains completely as at that temperature the contact angle between WC and Co is 0°. Thus at least for the hardmetals sufficiently rich in Co, a Co skeleton forms in the sintered products in addition to carbide skeleton. Hinnubar and Rudiger[17] explained that the high anisotropy of the hexagonal WC crystals leads the solid/solid interfacial energy lower along certain planes than the solid/liquid one and thus leading to direct contact between carbide grains.

Due to scarcity of Co, some alternatives are also tried as the bonding metal. Though Co is by far the best suitable bonding metal but still efforts are made to replace it by other transition metals like Ni or Fe.

I.4.1 Ni Substitution

From the introduction of cemented carbides in 1926, cobalt has been the traditional and predominant binder metal for tungsten carbide, although nickel and iron are cited as alternative. The reasons why nickel has not been used commercially

are somewhat confused. Dawihl[43] indicated that cobalt is preferred to nickel because cobalt has superior comminution characteristics and hence a better distribution of cobalt is achieved on the WC particles during milling, which subsequently leads to a better skeletal structure being formed during sintering. However, Dawihl[43] did indicate that nickel bonded alloys equivalent to cobalt bonded alloys can be obtained by using nickel oxide in place of nickel, since nickel oxide has comminution characteristics more akin to those of cobalt. Another reason given for the poor properties of the nickel bonded alloys is that the solubility of WC in Ni and Co is different. At high temperatures WC has a higher solubility in Co than Ni[44] but at low temperatures the reverse is true.[45] Other researchers[43,46] disagree, they state that the solubility at high temperatures is about the same, particularly in presence of excess carbon w_thin the stipulated range for hard-metal compositions. Nickel is said to be more prone than cobalt to the formation of brittle double carbides of the type $Ni_xW_yC_z$,[45,47] these carbides form when the Ni-W-C system is deficient in carbon. But Barlow[48] stated that nickel bonded WC alloys have similar properties to their cobalt bonded equivalents. Also there appears to be no major technical problems in their manufacture.

I.4.2 Fe Substitution

Efforts have been made to substitute Co in WC-Co system by another transition metal like Fe. Rautallea et.al.[49]

found out the phase diagram of Fe-W-C system according to which the maximum solubility of WC in Fe at 1250°C is 7.5%.

For Fe substitution through higher bending strength can be obtained but T.R.S. is only 40-60% to that of Co bonded WC. Moskowitz et.al.[50] found that for Fe substitution presence of η or graphite phase is also possible due to variation in carbon content in Fe. When the C content is between 0-1.4% then there is free η (Fe_3W_3C) phase while when C content is between 1.4 to 3.0% the system is free of graphite phase. It has been studied by them that upto the 0 to 1.4% C content in Fe, the hardness decreases with carbon content while between C content of 1.4 to 3.0% the hardness values increases and again when the C content exceeds 3.0%, it falls drastically.

I.4.3 Fe-Ni Substitution

Iron-nickel bonded tungsten carbide materials have not as yet been commercially applied, despite the fact that they are superior to the cobalt-bonded variety in transverse rupture strength as well as in resistance to abrasive wear. The remarkable strengths achieved by compositions of this system,[50] in the range of 420 to 455 Kg/mm^2 (600 to 650 KPSi), overshadow to some degree the system's superiority in abrasion resistance. However, the latter property may even be more significant than the strength in terms of potential for industrial application. In any case, the combination of superior strength and wear resistance indicates a high potential for their commercial utilization.

Moskowitz[51] observed that the abrasive wear resistance and hardness of Fe-Ni bonded WC is at a maximum at a binder Ni content of 10 weight percent, due to a peak in the amount of martensite at this composition.

I.5 Scope of the Present Investigation

Cobalt has been used quite successfully as the binder for WC based hardmetals for the last 50 years. But high cost and limited resources of the binder metal for the production of cemented carbide has led to investigate the possibilities of replacing the conventional constituents of hardmetal through other promising elements. It is well known that other transition metals such as nickel or iron show reasonably good bonding with WC and hence they can be used as the partial or complete substitution of Co in the traditional hardmetals. It is also interesting to see the possibilities of using Fe-Ni as binder for WC based hardmetal.

Lastly as straight WC-Co is not universally applicable for all cutting applications, the role of refractory compounds additives is an important one. The compounds selected presently are TiC, TiC-Mo_2C, TiN and TiB_2. The properties would certainly be influenced by the nature of bonding in the compound as well as its compatibility with the binder metal.

CHAPTER - II

EXPERIMENTAL PROCEDURES

The detailed experimental procedures carried out in the present investigation are presented in this chapter.

II.1 Raw Powder Characteristics:

The powders used in the experiments are having the following characteristics.

II.1.1 WC Powder

Supplier: General Electric, Cleveland (U.S.A.)

Average particle size: 0.78 μm (FSSS)

Size distribution:

Micron range	wt %
0-1	64.5
1-2	14.1
2-3	11.7
3-4	7.7
4-5	2.0

Chemical analysis

Mo	18 ppm
Fe	61 ppm
Cr	13 ppm
Ni	2 ppm
O	1036 ppm
C	Total 6.13%
	Free 0.04%

II.1.2 Cobalt Powder

Supplier: H.C. Starck, W. Germany

Average particle size: 2.3 μm (FSSS)

Chemical analysis

Ni	0.2%
Fe	0.04%
O	3500 ppm
Co	Balance

II.1.3 Nickel Powder

Supplier: INCO (U.K.) Type 123

Average particle size: 3.7 μm (FSSS)

Apparent density: 1.6 gm/cc

Surface area: 0.3 m^2/gm

Chemical composition (wt %)

C	0.06
Co	0.0003
Fe	0.005
O	0.05
N_2	0.003
S	0.0003
Other element	0.001
Ni	Balance

II.1.4 Iron Powder

Supplier: GAF Corporation (U.S.A.)

Average particle size (FSSS): 3-4 μm

Chemical composition

Fe	98.0 min
C	0.8 max
O	0.3 max
N	0.9 max

II.1.5 TiC Powder

Supplier: Treibacher Chemische Werke, Austria

Average particle size: 3.45 μm (FSSS)

Chemical composition:

C total	19.40%
C free	0.08%
Fe	0.05%
O	0.06%
Ti	Balance

II.1.6 60% TiC-40% Mo_2C Solid Solution

Supplier: Treibacher Chemische Werke, Austria

Average particle size: 4.8 μm (FSSS)

Chemical composition:

C total	14.18%
C free	0.05%
Fe	0.05%
O	0.13%
Mo_2C	39.9%
TiC	60.1%

II.1.7 TiN Powder

Supplier: Hermann. C. Starck, W. Germany

Average particle size: 7.2 μm (FSSS)

Apparent density: 1.54 g/cc

Chemical composition:

N	21.9%
C	0.3%
Ti	Balance

II.1.8 TiB_2 Powder

Supplier: H.C. Starck, W. Germany

Average particle size: 9.5 μm (FSSS)

Apparent density: 1.72 g/cc

Chemical composition:

B	30.3%
C	0.3%
O	0.25%
N	0.39%
Ti	Balance

II.1.9 Ni_2P Powder

Supplier: Alpha Products, U.S.A.

Average particle size: 5-7 μm (FSSS).

II.2 Premix Preparation:

The premix of carbides and metals were prepared by conventional ball milling technique. The powders were screened through 200 mesh seive before feeding in the ball mill for milling. The required amount of metal (Co, Ni, Fe) and carbide (WC, TiC etc.) powders were weighed in appropriate proportion on a single pan balance having accuracy upto 0.0001 gms. Wet milling of the powders in acetone was performed in a Fritsch 'Pulverisette-5' planatory type ball mill using 1.8×10^{-2} m diameter WC balls in acetone medium for 24 hrs. The ratio of feed to ball by mass was kept at 1:2. The milled premix was dried in open air.

The milled powders were manually mixed for 1 hr with 1% wax dissolved in benzene so as to provide green strength in the compacts.

II,3 Powder Characterisation:

The as received ball milled powders were characterised in terms of particle size and size distribution using Coulter Counter Analysis.

The method is based on the measuring the change in electrical resistance when particles suspended in electrical conducting liquid pass one by one through a small apperture in the liquid on either side of which electrodes are mounted. The change in resistance produces a voltage pulse which is proportional to the particle volume. Particle size determined by this method is therefore defined by the cube root of particle volume. In the present investigation NaCl and glycerol were used as electrolyte for the coulter counter analysis on model Z_B and B.

II.4 Compaction:

From the ball milled powder premix rectangular green compacts of 24.7 x 7.7 x 6.2 mm^3 (approximately) were prepared in a single acting hydraulic press at 350 MPa. This was necessary so as to give a uniform green density (50% theoretical density) for all the compositions, with varying binders. The green density of the green compacts were approximately 8 gm/cc. Manually operated hydraulic press (Apex Construction Ltd., U.K.) of 20 tonnes capacity was used for this purpose. The die made of high chromium high carbon steel and lined with WC, was cleaned with acetone and was lubricated with Zn-stearate prior to powder filling for each compaction.

The dimensions of the green pellets were measured with a vernier callipers (L.C = 0.001 cm) from which the volume of the pellets were calculated. Their weights were also measured using a single pan Mittler automatic (L.C = 0.0001 gm) balance. From the weights and volume of the pellets obtained, densities were calculated.

II.5 Presintering:

Furnace description - The furnace used was a resistance type. The heating elements being four silicon carbide (globar) rods. The furnace tube was made of inconel and was of 5 cm diameter and 90 cm length. The furnace rating was 1.8 KVA. It had a constant temperature zone of 10 cms at temperature ranges from 600-800°C. The temperature of the furnace was measured by a platinum/platinum-10% Rhodium thermocouple. The heating rate of the furnace was controlled with the help of a dimmerstat voltage regulator which controlled the voltage across the heating elements.

Hydrogen was passed through furnace, in order to maintain a reducing atmosphere within the furnace during pre-sintering. The gas was dried and cleaned by passing through a purification train before passing it into the furnace. The hydrogen purification train contained tubes containing calcium chloride for drying and glass wool, cotton etc. for removing any suspended particles. The hydrogen being an explosive gas, the furnace tube was sealed with heat resistant silicone adhesive in order to prevent hydrogen from coming into contact with air at elevated temperature.

Dewaxing of the green samples was carried out in the tubular furnace at 700°C for 1 hr, under hydrogen atmosphere. The purpose is to purge out the wax used as a lubricant during compaction. After allowing the presintered pellets to be furnace cooled their physical dimensions were measured.

II.6 Sintering:

The furnace described earlier was also used for sintering. Only the inconel tube was replaced by an Al_2O_3 tube of 5 cm diameter and 75 cm length. The furnace has a constant temperature zone of 5 cm at temperature ranges 1300-1400°C. Heating rate was 6.5°C/min.

Four green compacts at a time were kept on graphite boat packed with alumina powder and inserted in the centre of the furnace tube. Dry hydrogen gas (dew point - 35°C) was used as sintering atmosphere. T' e sintering temperature selected were 1350°C and 1400°C respectively and the sintering period was 1 hr.

The sintered pellets were furnace cooled and their dimensions, sintered densities, Vickers hardness, transverse rupture strength, magnetic properties were measured and the microstructure was examined. The microstructures revealed informations about the nature and amount of porosity, grain size and distribution of metal and carbide phases in the system.

II.7 Properties Evaluation:

The following sintered properties were measured from the sintered compacts.

II.7.1 Sintered Density

The sintered density of the sintered compacts were calculated from the mass and dimensional measurements of the samples. Sintered test pieces were impregnated with Xylene under vacuum and the following formula was used in order to calculate the sintered density

$$\text{Sintered density (gm/cc)} = \frac{\text{Weight of the compact in air (gm)}}{\text{Weight of xylene impregnated compact in air (gm)} - \text{Weight of xylene impregnated compact in water (gm)}}$$

Practically no difference was detected in the density values, obtained by either methods.

II.7.2 Densification Parameter

Densification parameter (ΔD) was expressed as follows:

$$\Delta D = \frac{\text{Sintered density} - \text{Green density}}{\text{Theoretical density} - \text{Green density}}$$

Theoretical density of WC was taken as 15.77 Mg/m^3 while for Co, Ni and Fe have been taken as 8.85, 8.9 and 7.84 Mg/m^3 respectively. Theoretical density of each composition was calculated from the simple rule of mixtures, taking the theoretical density of the various elements at room temperature.

II.7.3 % Sintered Porosity

To measure the % sintered porosity, first % theoretical density of the sintered test pieces was calculated and then deducted from 100.

$$\% \text{ theoretical density} = \frac{\text{Sintered density}}{\text{Theoretical density}} \times 100$$

II.8 Mechanical Tests:

II.8.1 Hardness

Hardness of the sintered compacts was measured on Vickers hardness testing machine Model HPO 250 of "Fritz Heckert" Leipzig make, using a load of 30 Kg. About eight indentations were taken on each polished specimen, and the average value was reported.

II.8.2 Transverse Rupture Strength

This test for 3-point loading was performed on a locally assembled apparatus, where the sintered hard metal bar was kept on two WC rollers of 3 mm diameter and 15 mm length which were 10 mm apart from each other. Another similar roller was kept in the middle of the bar. The load was applied gradually by a manually operated hydraulic press. A load gauge was attached to the measuring system. The maximum rupture load at the failure point of the test piece was used in the following formula in order to determine transverse rupture strength

$$\text{T.R.S. } (MN/m^2) = \frac{3 \times \text{Load (MN)} \times \text{Length (m)}}{2 \times \text{Width (m)} \times (\text{Thickness, m})^2}$$

II.9 Magnetic Properties:

Magnetic properties like coercivity and magnetic saturation have been measured to get an idea of the metal phase distribution in the sintered hardmetal. A Fritzsch make coercivity meter was used for this purpose.

II.10 Microstructural Studies:

II.10.1 Optical Microscopy

The selected sintered compacts were wet polished primarily on the diamond wheel. Then they were fine polished by the diamond powders of decreasing size ranges viz. 20-10 μm, 10-5 μm and below 5 μm. Diamond powders in suspension were spread on the backside of the hard photographic papers which were fixed on a wheel and rotated at slow speed.

The unetched polished samples were observed under the optical microscope with a magnification of 200X to get an idea of pore sizes and their distribution.

$FeCl_3$ dissolved in strong HCl was used as the etchant for the straight WC-metal hardmetals. For other samples Murakami's reagent was used. Etching period was maintained for 5-6 minutes. After etching the photographs of the optical microstructures were taken at a high magnification of 3000X.

II.10.2 Scanning Electron Microscopy

The photographs of fractured surface after T.R.S. test was taken at 1500X and 3000X to have an idea about the nature of fracture of the hardmetals investigated.

Scanning electron microscope model ISI-60 was used to observe the fracture surface of the failed samples after T.R.S. test. The mode of operation was SE and the operating voltage was 120 KV (SE secondary electrons).

II.11 Dilatometric Studies:

Dialatometric study of the hardmetals having varying binder composition was done to analyse the dynamic shrinkage during sintering. For this purpose the samples of size, 26 x 10 x 8 mm^3 (approximately) were prepared at 700 MPa. Inert atmosphere was maintained throughout the experiment by using dry argon gas. The pellets were heated to 1400°c at a heating rate of 5°C/minute and then allowed to be furnace cooled to room temperature. Dilatometer used for this purpose was of Orton U.S.A. make with autorecording system.

II.12 Oxidation Studies:

Oxidation of 90 WC-10 (Co/Ni) hardmetals sintered at 1400°C for 1 hr was done to study the oxidation behaviour. The specimens of 6 x 4 x 3 mm^3 (approximately) were machined from the sintered compacts. These were subsequently polished. Isothermal weight gain measurements were made on a continuous recording semimicro balance (Anisworth, U.S.A.) with a Bristol Recording system. The sample was suspended from the pan of the balance and was allowed to oxidise in air. The test temperature was 800 $\pm$ 5°C accuracy and the test was carried out for periods up to 8 hrs. The time was recorded on the Y axis and the weight gain on the X axis of the automatic recording chart of the system.

After oxidation, X-ray diffraction of the oxide surfaces was performed with a Rich-Seifert (Germany) X-ray

diffractometer. Changes in weight per unit surface area (ΔW) have been used for quantitative calculation. A general equation for any oxidation process is expressed as $(\Delta W)^n = Kt$, where ΔW is change in weight per unit surface area, K is the rate constant, t is the time, and n is the power index which indicates any particular law.

CHAPTER III

EXPERIMENTAL RESULTS

This chapter describes the results of milled premix powder characterisation and sintering studies. Part I describes the results of WC-10 Co hardmetals with binder substitution while Part II and III describe the results of WC-10 Co hardmetals with refractory compounds and Ni/Ni_2P additions respectively.

III.1 Powder Premix Characterisation:

The preparation of composite premix powders was done using mechanical milling. It was observed that the average particle size of the as received powder has not got reduced much over 24 hrs milling (Table 3.1). For particle size distribution coulter counter analysis values are also reported (Table 3.2).

Table 3.1 Average particle size of the as received and mechanically milled powders after FSSS analysis

Powders	Condition	Average particle size (μm)
WC	As received	0.78
Ni	"	2.30
Co	"	3.70
Fe	"	3.50
TiC	"	3.45
60% TiC - 40% Mo_2C (solid solution)	"	4.80
TiN	"	7.20
TiB_2	"	9.50
WC-10% Co	24 hrs milled	0.80
WC-10% binder (75 Co/25 Ni)	"	0.87
WC-10% binder (50 Co/50 Ni)	"	0.81
WC-10% binder (25 Co/75 Ni)	"	0.84
WC-10% Ni	"	0.76
WC + 10% binder (75 Co/25 Fe)	"	0.74
WC + 10% binder (50 Co/50 Fe)	"	0.83
WC + 10% binder (25 Co/75 Fe)	"	0.81
WC + 10% Fe	"	0.76
WC + 10% binder (75 Ni/25 Fe)	"	0.79
WC + 10% binder (50 Ni/50 Fe)	"	0.74
WC + 10% binder (25 Ni/75 Fe)	"	0.80
WC + 10% Co + 5% TiC	"	0.87
WC + 10% Co + 10% TiC	"	0.85
WC + 10% Co + 5% TiC-Mo_2C (solid solution)	"	0.79
WC + 10% Co + 10% TiC-Mo_2C (solid solution)	"	0.82
WC + 10% Co + 5% TiB_2	"	0.78
WC + 10% Co + 10% TiB_2	"	0.75
WC + 10% Co + 5% TiN	"	0.72
WC + 10% Co + 10% TiN	"	0.76

Table 3.2 Particle size distribution after coulter counter analysis of mechanically milled powders

Powder composition	Micron ranges				
	0-1	1-2	2-3	3-4	4-5
WC + 10% Co	72.1	15.8	4.3	3.6	4.2
WC + 10% binder (75 Co/25 Ni)	70.5	19.8	3.6	2.0	4.1
WC + 10% binder (50 Co/50 Ni)	79.9	8.4	3.7	6.5	1.5
WC + 10% binder (25 Co/75 Ni)	68.6	9.8	10.5	6.4	4.7
WC + 10% Ni	70.1	12.3	7.1	6.3	4.2
WC + 10% binder (75 Co/25 Fe)	69.2	16.2	8.3	4.3	2.0
WC + 10% binder (50 Co/50 Fe)	74.1	12.4	6.5	4.2	2.8
WC + 10% binder (25 Co/75 Fe)	71.9	13.8	7.2	6.2	0.9
WC + 10% Fe	78.2	9.7	4.3	3.7	4.1
WC + 10% binder (75 Ni/25 Fe)	67.7	13.8	3.7	10.5	4.3
WC + 10% binder (50 Ni/50 Fe)	70.4	11.5	8.2	6.3	3.6
WC + 10% binder (25 Ni/75 Fe)	72.3	14.3	6.3	3.6	3.5

PART I

III.2 Sintering of WC-10 Co/Ni/Fe Composites:

III.2.1 Densification Behaviour

It is apparent from Figure 3.1 that sintered density of WC-10 Co hardmetal generally decreases with increase in the Ni content with the exception of 1350°C sintering for 50 Co/50 Ni binder. Further, with increase in the sintering temperature the sintered density increases. Such a trend has also been confirmed by porosity and densification plots (Figure 3.1).

Sintered density of WC-10 Co hardmetal also decreases with increase in the Fe content followed by increase in density at higher Fe content in binder (Figure 3.1). But in this case the decrease in density is not so drastic like WC-10(Co/Ni) hardmetals. The increase in sintering temperature from 1350°C to 1400°C causes increase in sintered density for all the compositions. Densification parameter also follows the same trend as that of density and it is close to unity for most of the WC-10(Co/Fe) hardmetals after 1400°C sintering. The noticeable feature in this case is that the nature of the plot does not change with increase in sintering temperature from 1350°C to 1400°C. The porosity plot also follows the same nature as to that of density and densification plots (Figure 3.1).

Figure 3.1 shows that the sintered density of WC-10(Ni/Fe) hardmetal follows a sinusoidal curve showing maxima at 25 Ni/75 Fe binder composition. It has been observed in the

figure that sintered density does not vary appreciably with increase in Fe content in binder from 75% to 100%. It is also evident from the figure that straight WC-10 Ni has got the lowest density over other binder compositions. The densification parameter and porosity have a similar trend of variation like sintered density.

Comparing all the systems shown in Figure 3.1 it is clear that in majority WC-10(Ni/Fe) hardmetal shows better densification behaviour than that of either WC-10(Co/Ni) or WC-10(Co/Fe) hardmetal as well.

III.2.2 Dilatometric Studies

Figures 3.2 to 3.4 show the variation of percent linear shrinkage of hardmetals with temperature when sintered at 1400°C in argon. All the plots show initial expansion in length followed by shrinkage. Figure 3.2 shows that early densification occurs in case of WC-10 Co hardmetal among all WC-10(Co/Ni) hardmetals. But the densification behaviour of 25 Co/75 Ni hardmetal is noticeable. Initially the densification for the latter is better than other compositions, but it becomes slower when the temperature becomes closer to 1400°C. Similar features are observed for hardmetals containing 25 Co/75 Fe, 100 Fe, 50 Ni/50 Fe and 25 Ni/75 Fe binders.

From Figures 3.2 to 3.4 it is evident that maximum linear shrinkage obtained in case of WC-10 Co hardmetal, but after substitution of the binder with Ni/Fe or Fe(25%) shows maximum linear shrinkage.

III.3 Mechanical Properties:

III.3.1 Hardness

Figure 3.5 shows that hardness of the sintered hardmetals decreases with increase in Ni concentration in the binder which is correlable with the densification plots (Figure 3.1). Further, an increase in sintering temperature from 1350 to 1400°C resulted in increase in hardness for all the compositions, although the variation trend remained unchanged.

For WC-10(Co/Fe) hardmetal after 1350°C sintering, hardness decreases with increase of Fe content followed by increase at higher Fe content. However, an increase in sintering in sintering temperature to 1400°C gives better result.

It is evident from Figure 3.5 that in WC-10(Ni/Fe) hardmetal, the hardness value increases with increase in Fe content and remains almost constant at higher Fe content. Among all the systems studied WC-10(Ni/Fe) system gives a constant hardness over a range of binder compositions.

III.3.2 Transverse Rupture Strength (T.R.S.)

T.R.S. values of sintered WC-10(Co/Ni) hardmetals (Figure 3.5) steadily decreases with increase in Ni content except in case of 50 Co/50 Ni binder composition. WC-10 Ni shows the minimum T.R.S. The nature of variation of the plots is similar to the hardness variation (Figure 3.1).

T.R.S. values of WC-10 (Co/Fe) hardmetals (Figure 3.5) decreases drastically with increase in Fe content except for

100% Fe binder compositions. Here the T.R.S. curve passes through a minimum at 25 Co/75 Fe binder composition.

In case of WC-10(Ni/Fe) hardmetals, the T.R.S. values first increase with increase in Fe content and then decrease with a moderate recovery at 100% Fe binder composition, such that the plot shows a maximum at 50 Ni/50 Fe binder composition.

Among all the substitutions, hardmetals containing 50 Ni/50 Fe binder show maximum T.R.S. value and is close to the T.R.S. value of WC-10 Co hardmetal.

III.4 Magnetic Properties:

Magnetic properties such as coercivity and magnetic saturation were studied and values are reported (Figure 3.6) to get an idea about the binder phase distribution in the system. Coercive force of WC-10(Co/Ni) hardmetal decreases with increase in Ni content and ultimately reaches a zero value with the exception of 50 Co/50 Ni binder composition. The magnetic saturation curve follows the same trend as to that of coercive force. But for WC-10(Co/Fe) hardmetal, the coercive force increases upto 50% Co substitution followed by continuous decrease. Magnetic saturation shows continuous increase upto 100% Fe such that the values are almost constant over all the binder composition except for WC-10 Co. For WC-10 Ni hardmetals, the coercive force initially decreases with increase in Fe followed by an increase. Magnetic saturation variation in WC-10(Ni/Fe) systems is more or less identical to WC-10(Co/Ni) hardmetals.

III.5 Microstructure and Fractography:

The optical photomicrographs and scanning electron fractographs of WC-10(Co/Ni), WC-10(Co/Fe) and WC-10(Ni/Fe) hardmetals sintered at 1400°C for 1 hr in dry hydrogen are shown in Figures 3.7 to 3.10. As the alloy systems were of micrograin, shape of the grains is not very obvious from optical photomicrographs. However, scanning electron fractographs reveal a typical non plastic deformed structure of the surface. It is also evident from the scanning pictures that pores are also in general closed ones.

Grain size variation with binder compositions is reported in Figure 3.6. It shows that there is slight increase in grain size for WC-10 Co hardmetal with increase in either Ni and Fe in the binder. On the other hand, the grain size remains almost same in case of WC-10(Ni/Fe) hardmetals over all the binder compositions.

III.6 Oxidation Behaviour:

III.6.1 Weight Gain

The oxidation study of WC-10(Co/Ni) hardmetals (sintered at 1400°C, 1 hr, H_2) was carried out at 800°C in air. Linear plots of weight gain versus time are given in Figure 3.11. It shows that over all the binder compositions investigated, the change in weight with time is a minimum for the 100% Co binder, whereas hardmetals containing Co/Ni binder show less oxidation resistance. The nature of weight gain versus time plots is similar for all WC-10(Co/Ni) hardmetals.

From double log plot of weight gain versus time (Figure 3.12), the calculated 'n' values are between 1.5 to 2 for all WC-10(Co/Ni) hardmetals.

III.6.2 X-ray Analysis

The X-ray studies results show that the oxidised surfaces of all the hardmetals of system WC-10(Co/Ni) contained WC, tungsten oxide (WO_3), binder metal tungstates (BWO_4) and binder oxide (B_2O_3)in case of pure metal binder; however in case of all the alloy binders their corresponding oxides could not be detected. The results have been given in Appendix I.

PART II

Sintering of WC-10 Co Hardmetals with Refractory Compounds Addition

III.7 Densification Behaviour:

Figure 3.13 shows that sintered density falls steadily with increase in refractory compounds in WC-10 Co hardmetals, with the exception of TiC-Mo_2C addition which shows slight density increase after 10% addition. Figure 3.13 shows that with increase in TiC-Mo_2C addition the densification parameter increases. Among all the refractory compound additions TiB_2 addition shows worst densification.

III.8 Mechanical Properties:

III.8.1 Hardness

Effects of refractory compounds addition on the hardness values of WC-10 Co hardmetal have been reported in Figure 3.14.

It has been noticed that as the amount of TiC and TiC-Mo_2C addition is increased, the hardness decreases steadily. But in case of TiB_2 and TiN additions, hardness initially decreases drastically followed by an increase at higher additions. From Figure 3.14 it is evident that TiB_2 addition has worst effect on the hardness of WC-10 Co hardmetals.

III.8.2 Transverse Rupture Strength (T.R.S.)

Figure 3.14 shows that TiC, TiC-Mo_2C and TiN additions decrease T.R.S. of WC-10 Co hardmetals initially but increases again with further additions. However, in case of TiB_2 addition T.R.S. decreases drastically first and remains almost unchanged with its further addition.

III.9 Magnetic Properties:

Effect of refractory compounds additions on magnetic properties of WC-10 Co hardmetal has been reported in Figure 3.15. It has been shown that the addition of either of the refractory compounds TiC and TiN causes increase in magnetic saturation but at higher TiC addition, a decrease in coercivity is observed. The nature of variation of magnetic properties i.e. magnetic saturation and coercive force after TiB_2

addition are similar such that they first decrease and then increase at higher additions.

III.10 Scanning Electron Fractographs:

Scanning electron fractographs of WC-10 Co hardmetals with refractory compounds addition are shown in Figure 3.16. The deplex structure is evident showing bigger particles (in micron range) of the refractory compound additives.

The grain size (Figure 3.15) of WC-10 Co hardmetal marginally changes with the refractory compounds addition.

PART III

Sintering of WC-10 Co Hardmetals Containing Ni/Ni_2P

III.11 Densification Behaviour:

Sintered properties of WC-10(Co-Ni/Ni_2P) hardmetals are reported in Figure 3.17. It shows that the sintered density decreases with increase in Ni/Ni_2P in binder upto 50% substitution and after that increases steadily except 100 Ni/Ni_2P binder hardmetal for 1150°C sintering. Further, increase in sintering temperature results in higher density. Compared to the sintered density of WC-10 Co hardmetal (Figure 3.1) sintered density of WC-10(Co-Ni/Ni_2P) hardmetals is very poor. Densification parameter and porosity plots confirm the same fact.

III.12 Hardness:

The sintered hardness of WC-10(Co-Ni/Ni_2P) hardmetals has been reported in Figure 3.17. Hardness variation with binder composition remains unaltered after an increase in sintering temperature from 1150°C to 1250°C. But for 1200°C sintering it shows continuous decrease in hardness with slight recovery at 100 Ni/Ni_2P binder composition.

III.13 Magnetic Properties:

Coercive force of sintered WC-10(Co-Ni/Ni_2P) hardmetals is reported in Figure 3.17. It is evident from the figure that coercive force decreases with increase of Ni/Ni_2P in binder.

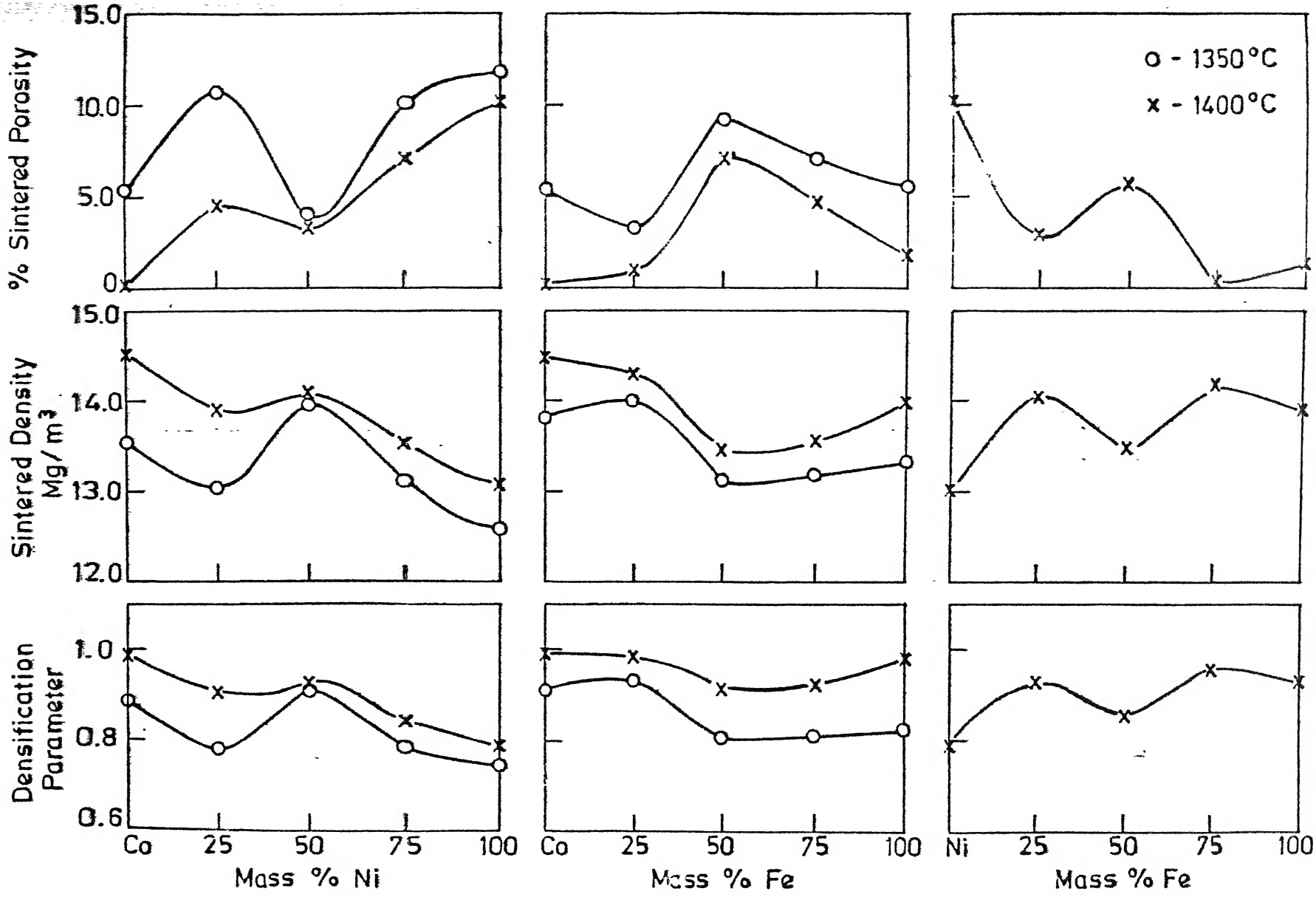

Fig. 3.1 Properties of WC-10 % (Co, Ni, Fe) hardmetals, sintered at 1350°C and 1400°C respectively for 1hr in dry H_2

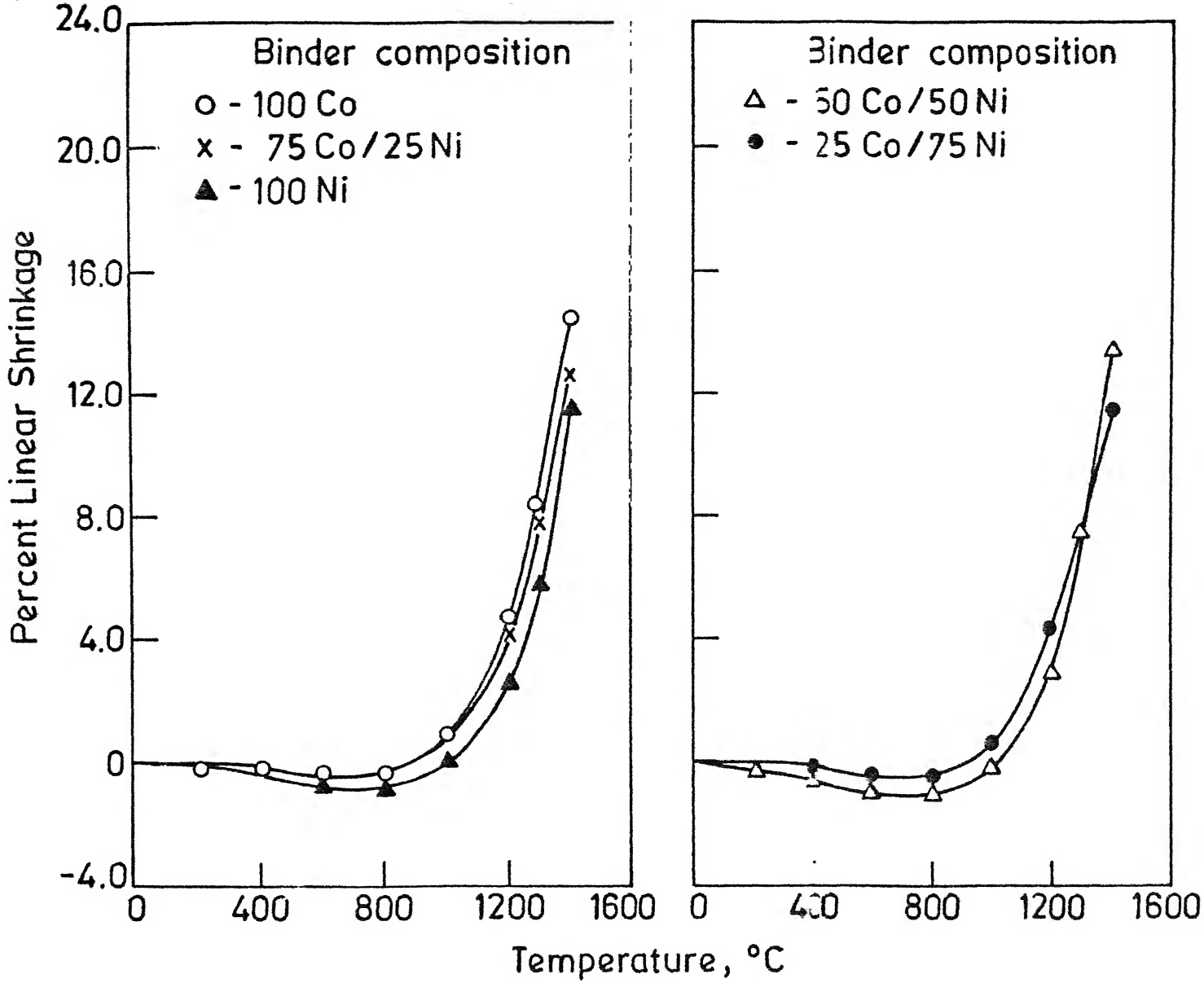

Fig. 3.2 Dilatometric plots of WC-10(Co/Ni) hard metals.

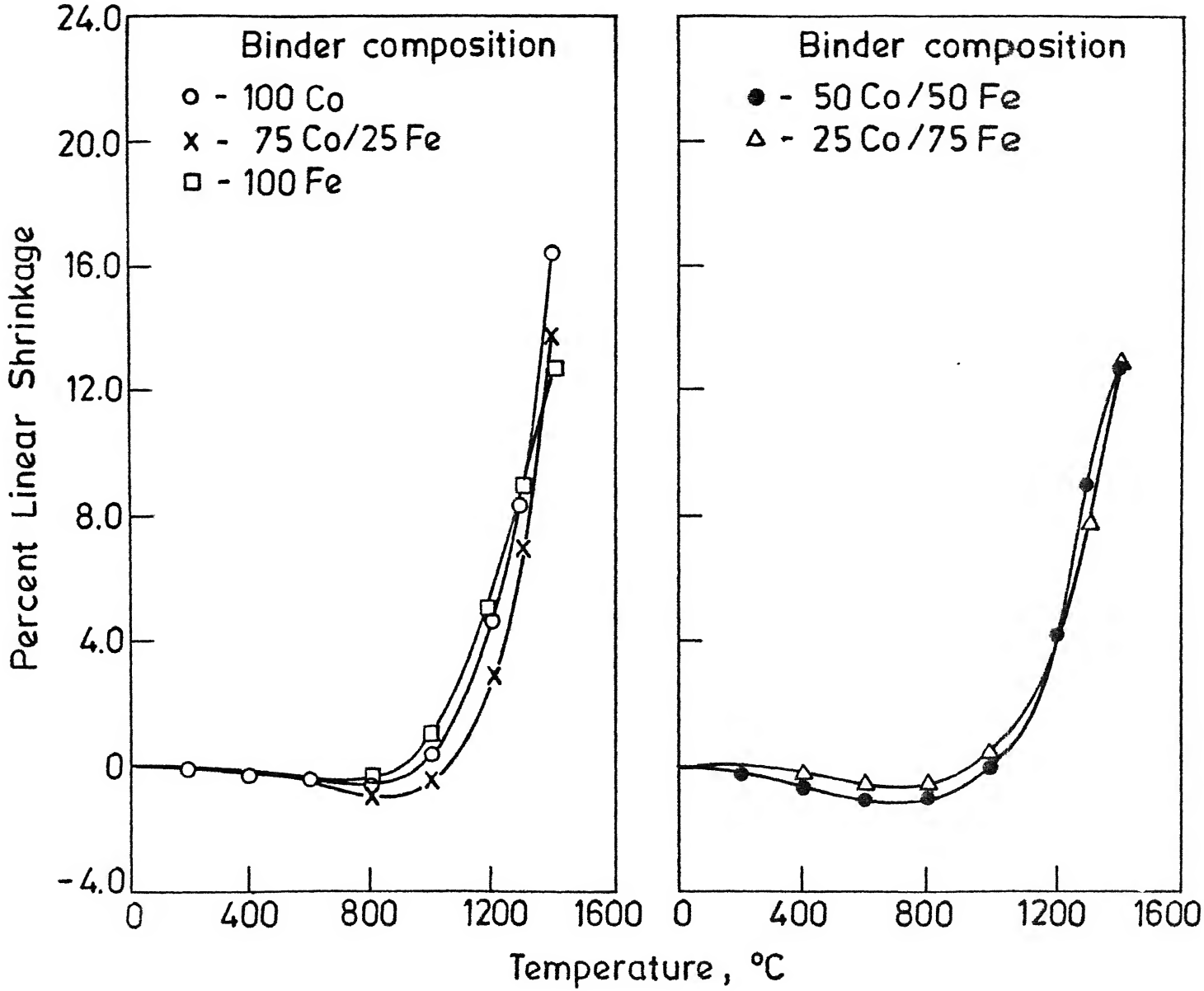

Fig. 3.3 Dilatometric plots of WC-10 (Co/Fe) hard metals.

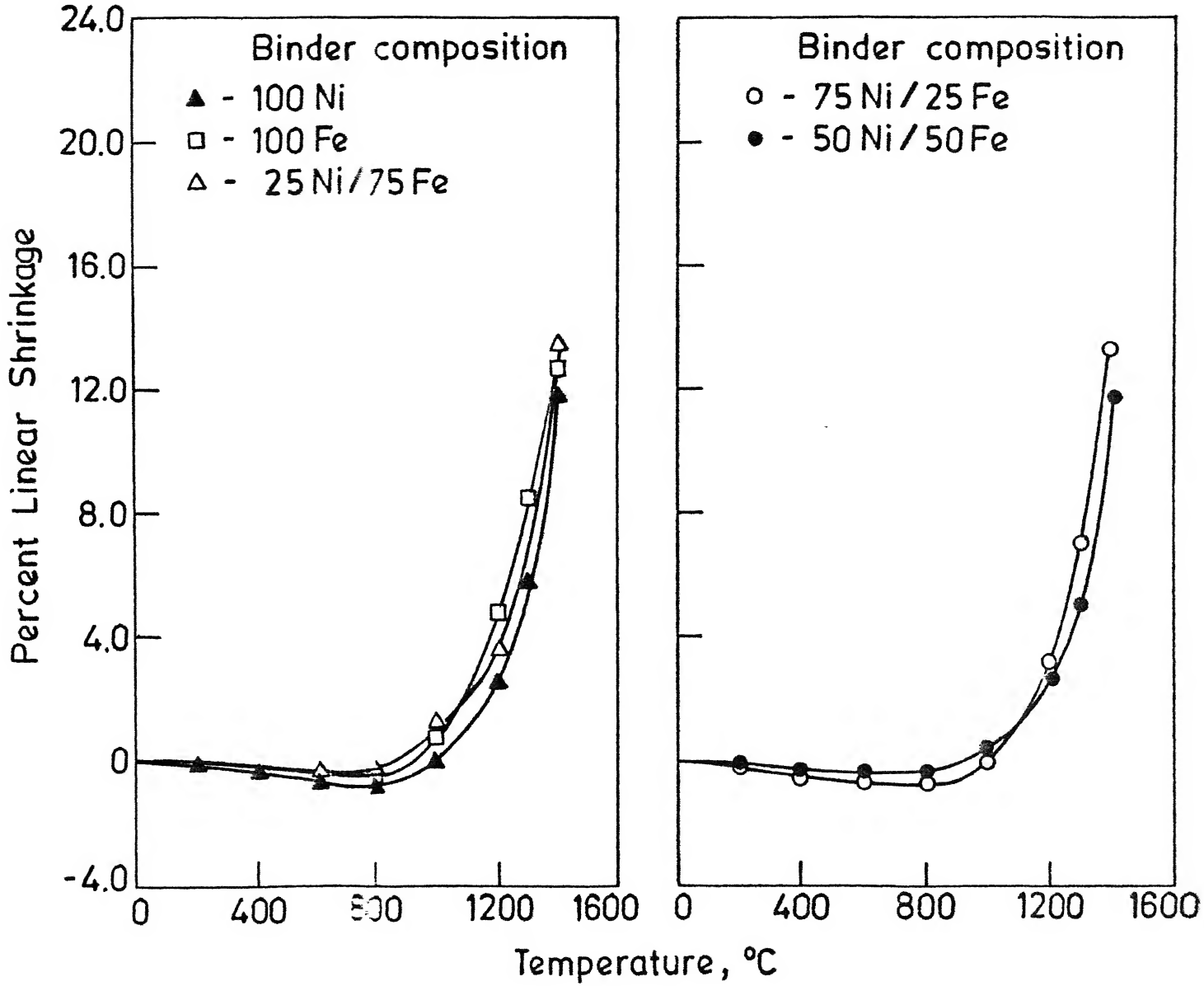

Fig. 3.4 Dilatometric plots of WC-10(Ni/Fe) hard metals.

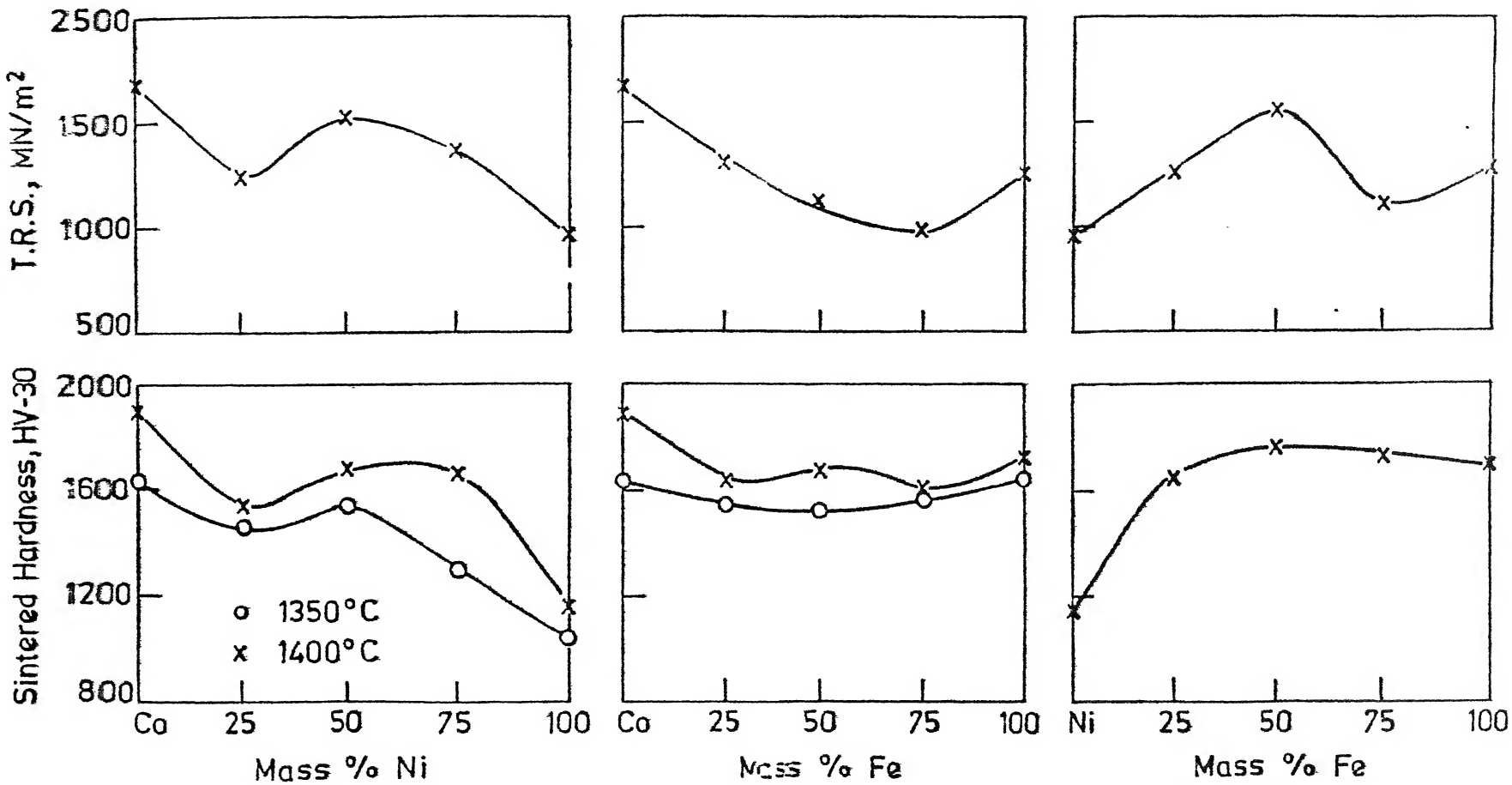

Fig. 3.5 Hardness and T.R.S. plots of WC-10% (Co, Ni, Fe) hardmetals, sintered at 1350°C and 1400°C respectively for 1hr in dry H_2.

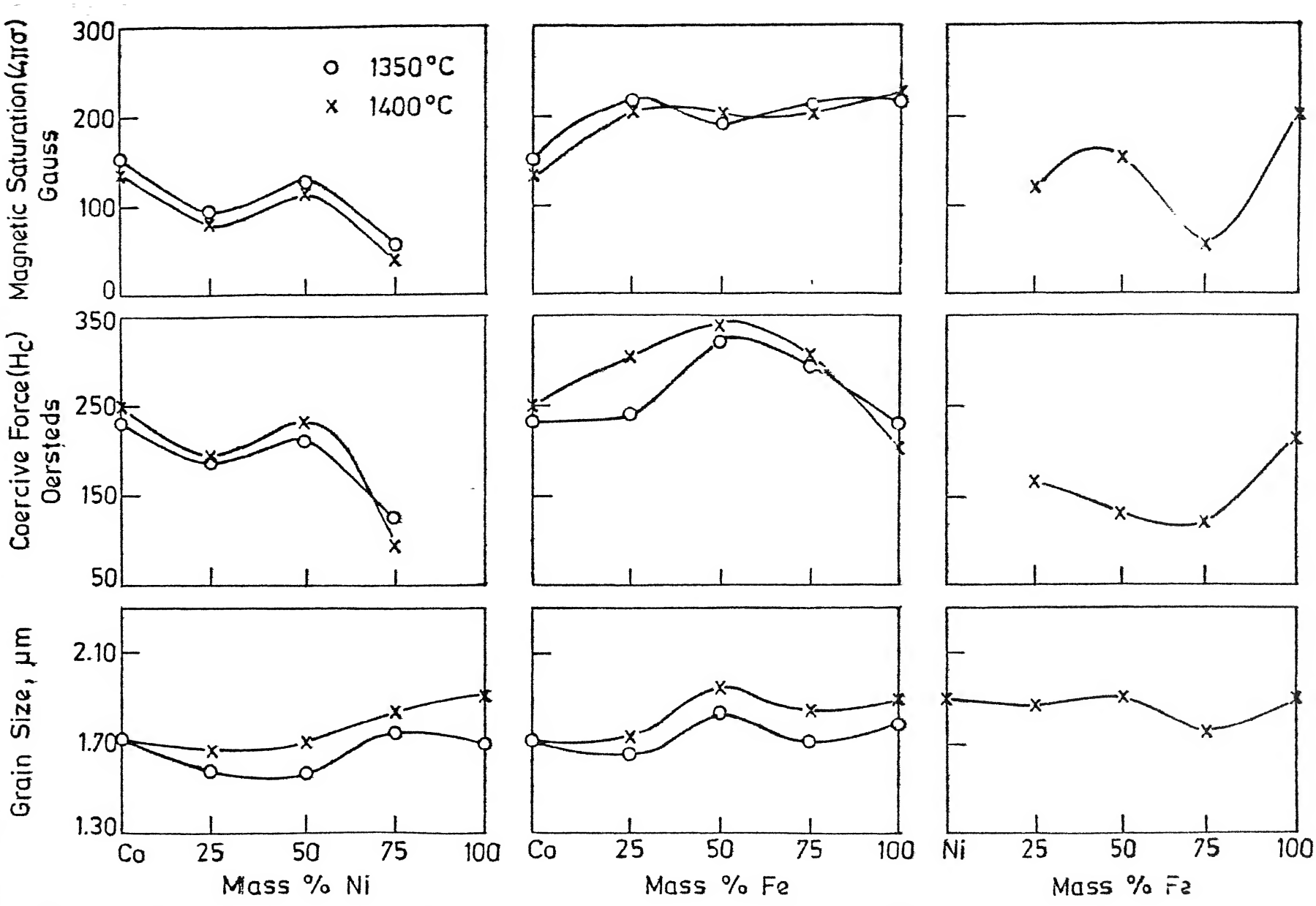

Fig. 3.6 Grain size and magnetic properties variation of WC-10% (Co, Ni, Fe) hardmetals, sintered at 1350°C and 1400°C respectively for 1hr in dry H_2

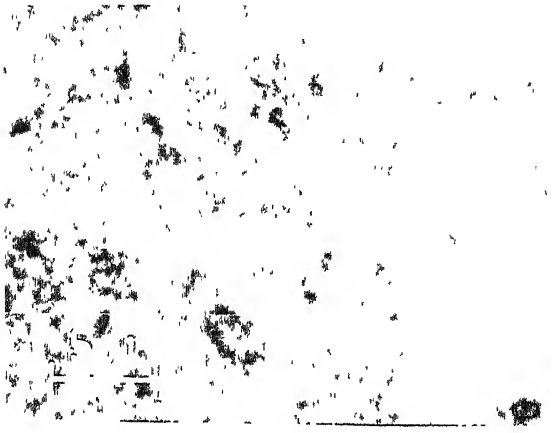

100 Co

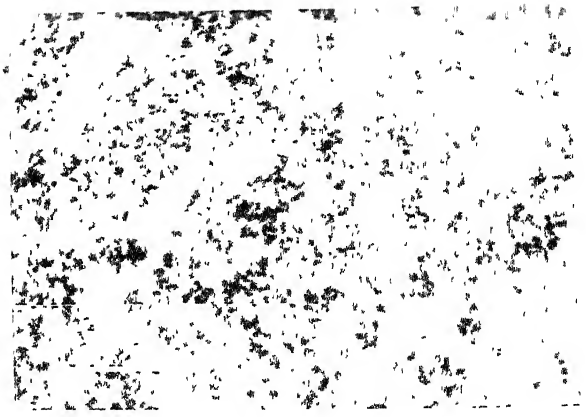

50 Co/50 Ni

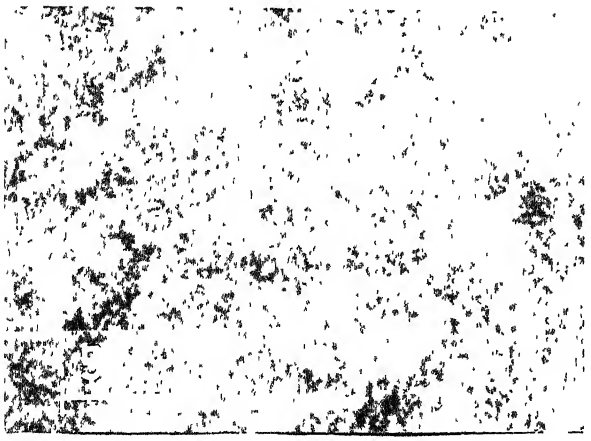

75 Co/25 Fe

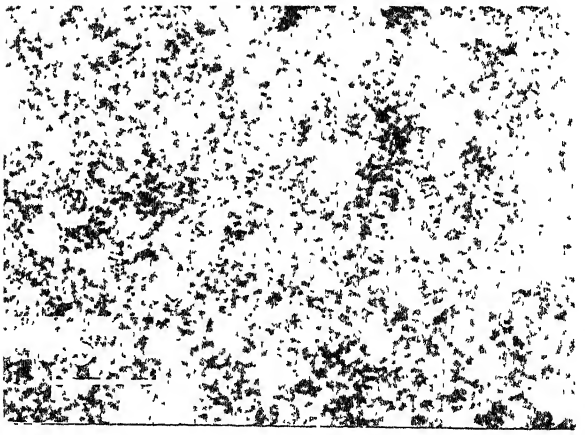

25 Co/75 Fe

Fig. 3.7 Some typical optical photomicrographs of WC-10(Co/Ni) and WC-10(Co/Fe) hardmetals with varying binder compositions sintered at 1400°C for 1 hr in dry H_2.

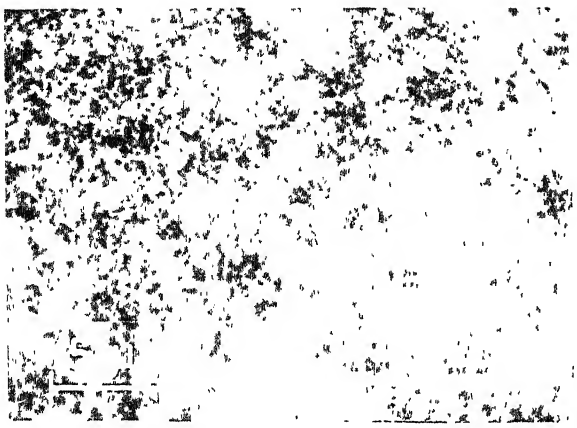

75 Ni/25 Fe

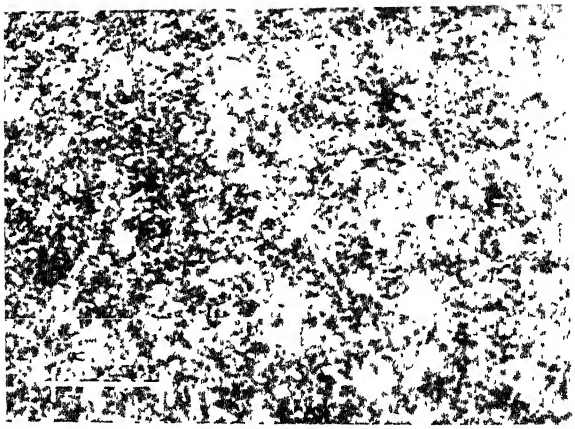

50 Ni/50 Fe

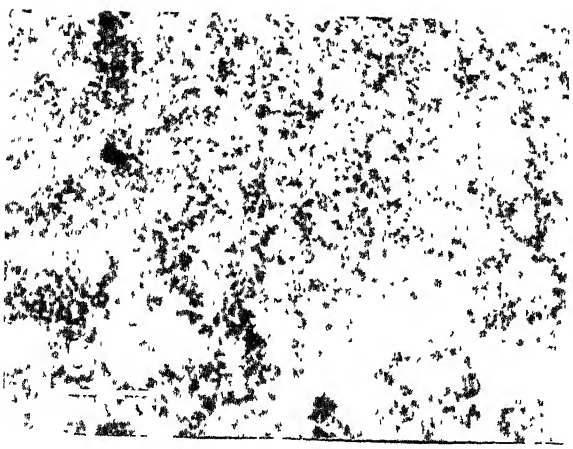

25 Ni/75 Fe

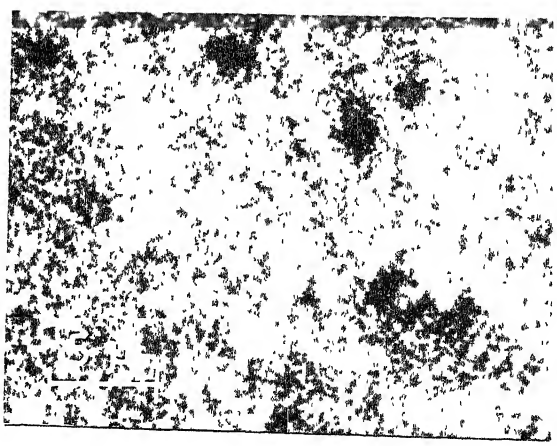

100 Fe

Fig. 3.8 Some typical optical photomicrographs of WC-10(Ni/Fe) hardmetals with varying binder composition sintered at 1400°C for 1 hr in dry H_2.

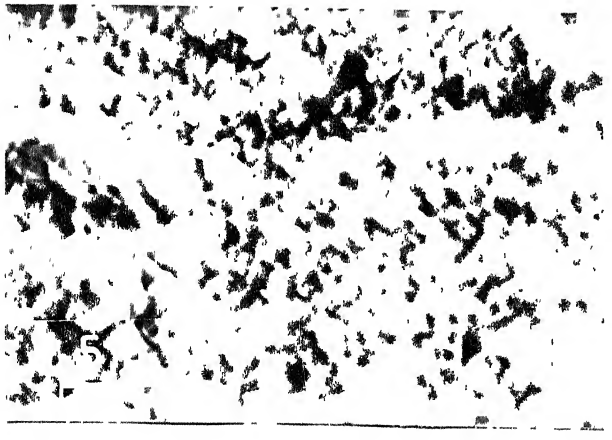

100 Co

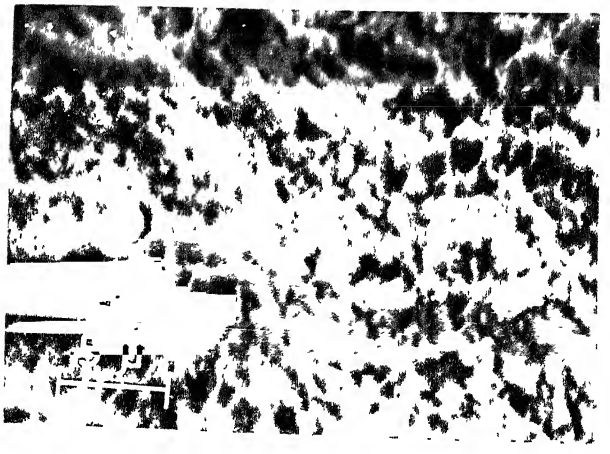

75 Co/25 Ni

50 Co/50 Ni

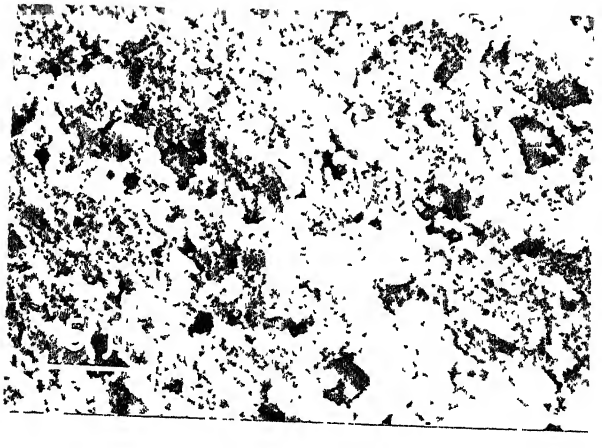

100 Ni

Fig. 3.9 Some typical scanning electron fractographs of WC-10(Co/Ni) hardmetals with varying binder composition, sintered at 1400°C for 1 hr in dry H_2.

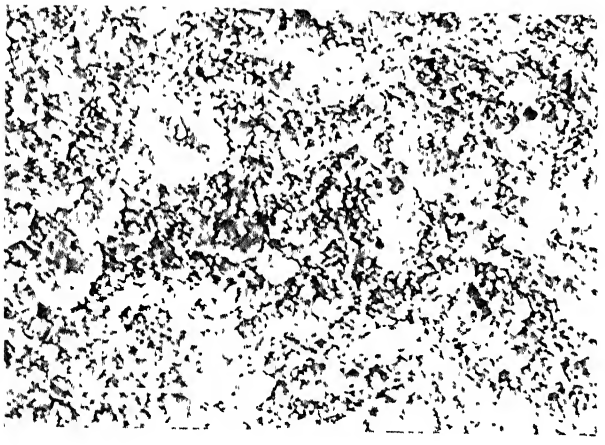

75 Co/25 Fe

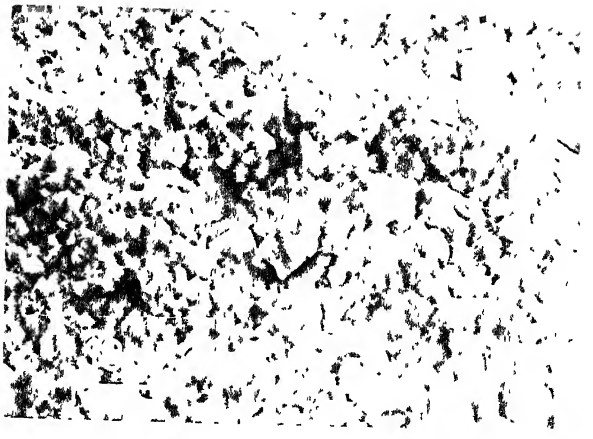

100 Fe

75 Ni/25 Fe

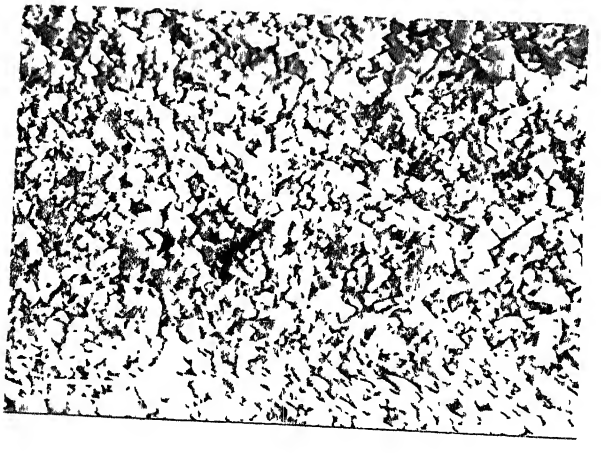

25 Ni/75 Fe

Fig. 3.10 Some typical scanning electron fractographs of WC-10(Co/Fe) and WC-10(Ni/Fe) hardmetals with varying binder composition, sintered at 1400°C for 1 hr in dry H_2.

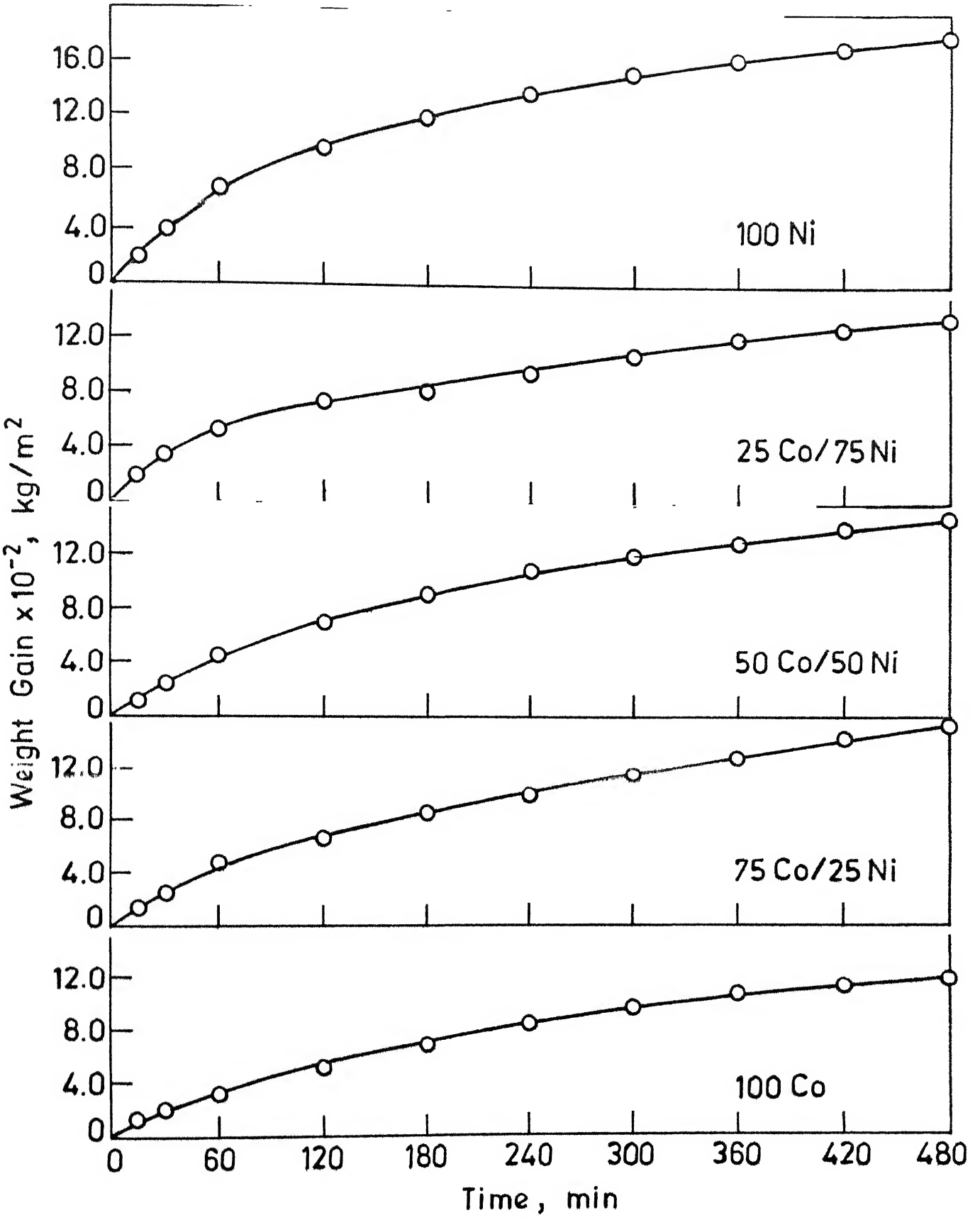

Fig. 3.11 Weight gain vs time plot of sintered WC-10(Co, Ni) hard metals after oxidation at 800°C in air.

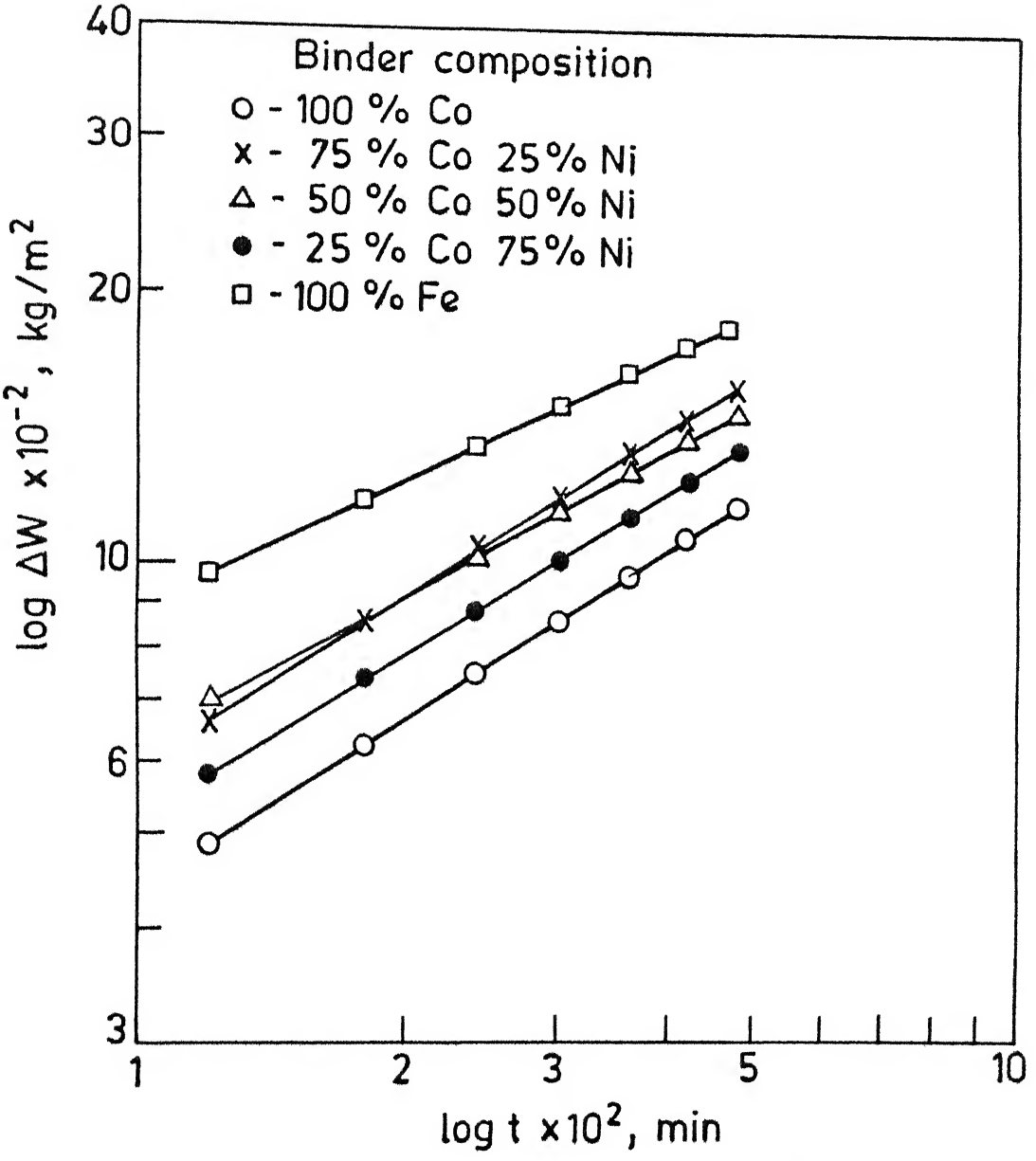

Fig. 3.12 Weight gain vs time (log scale) plot of WC-10% (Co, Ni) hardmetals, oxidized at 800°C air (sintering temperature 1400°C, 1hr, H_2)

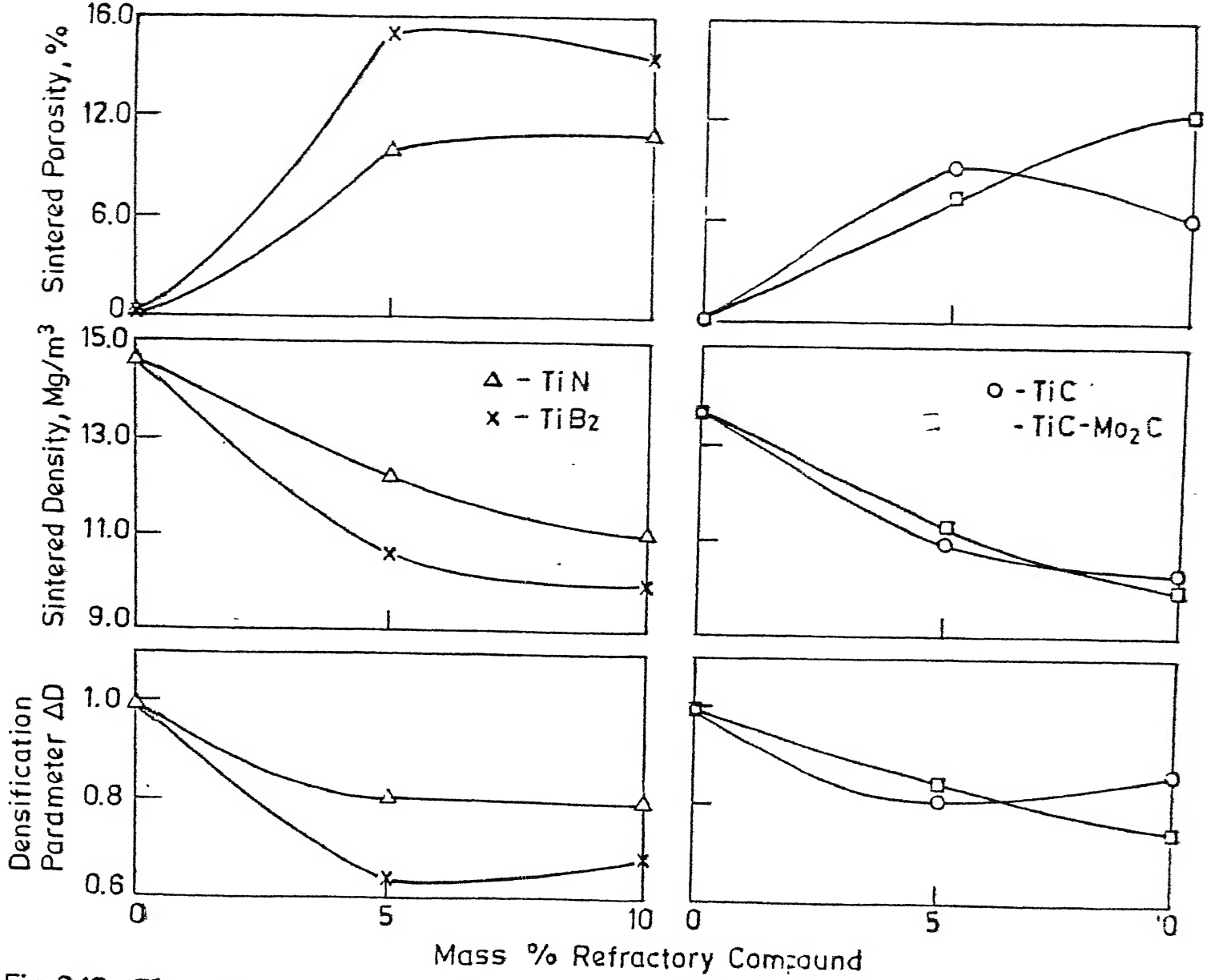

Fig. 3.13 Sintered properties of WC-10% Co hardmetals containing refractory compounds sintered at 1400°C for 1hr in dry H_2

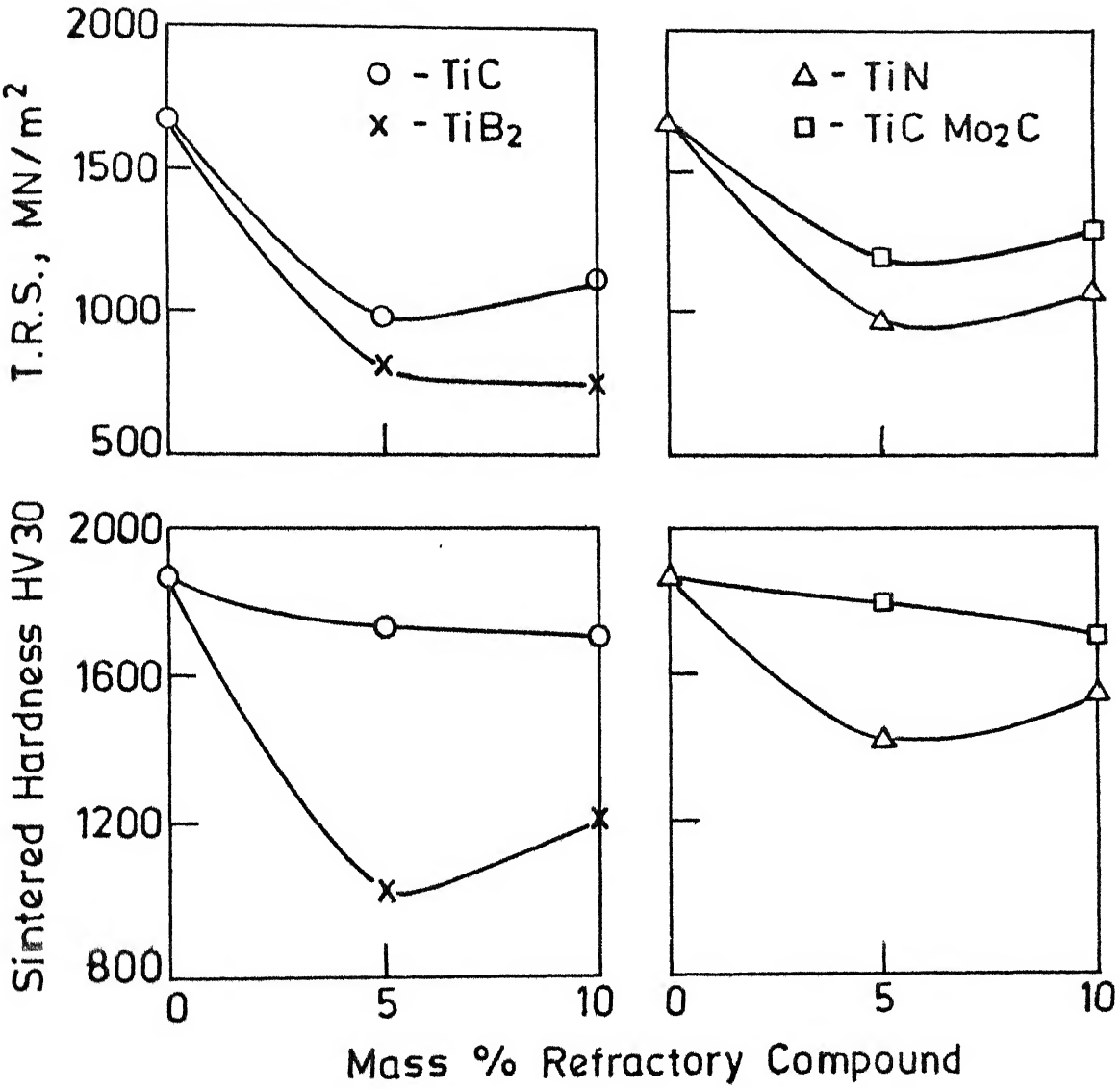

Fig. 3.14 Hardness and T.R.S. plots of WC-10% Co hard-metals containing refractory compounds, sintered at 1400°C for 1hr in dry H_2

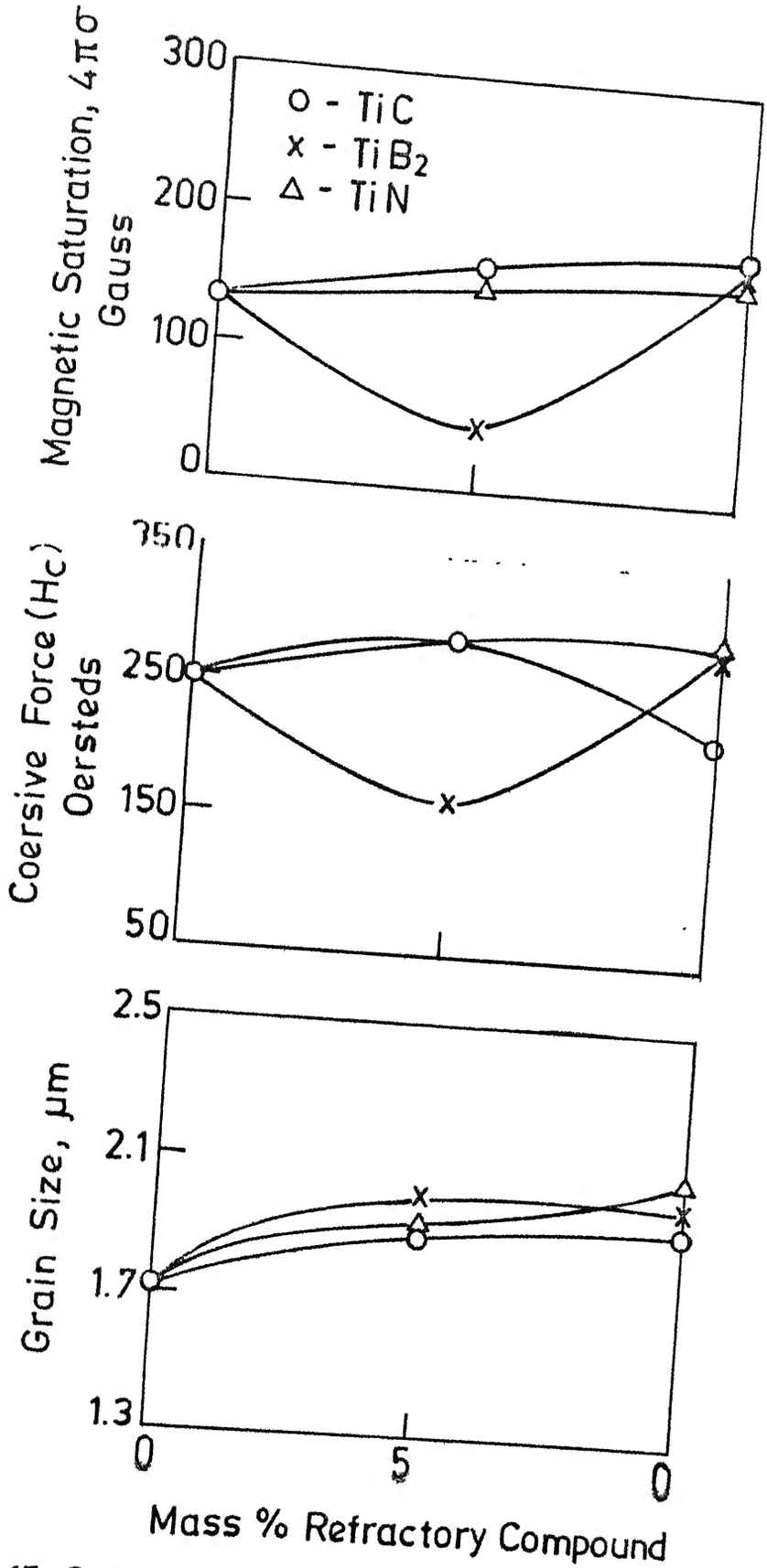

Fig. 3.15 Grain size and magnetic propeties variation of WC-10Co hardmetals containing refractory compound, sintered at 1400°C for 1hr in dry H_2.

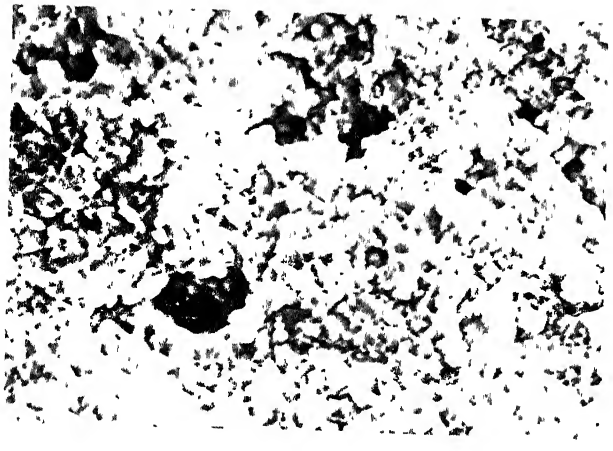

5% TiC-Mo_2C

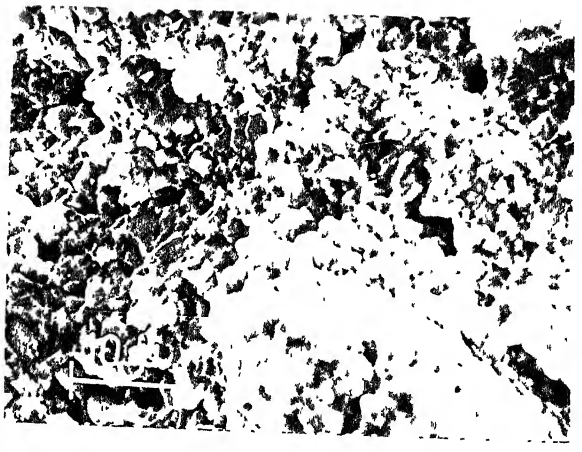

10% TiC-Mo_2C

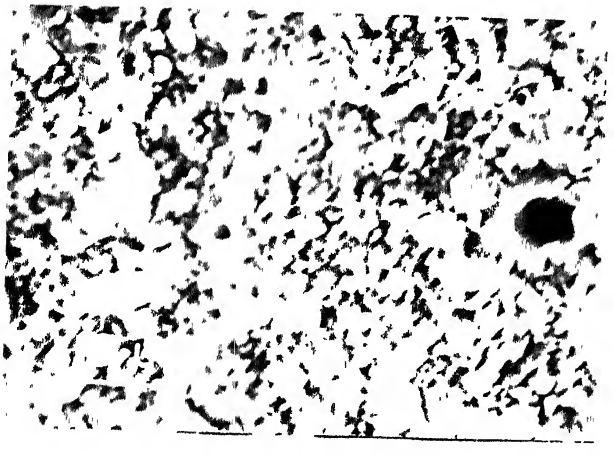

5% TiC

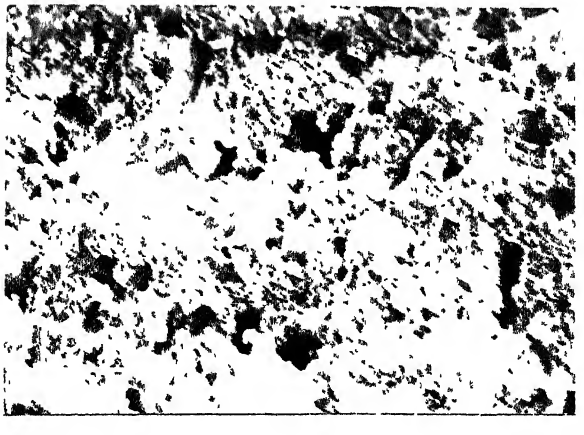

10% TiC

contd...

contd...

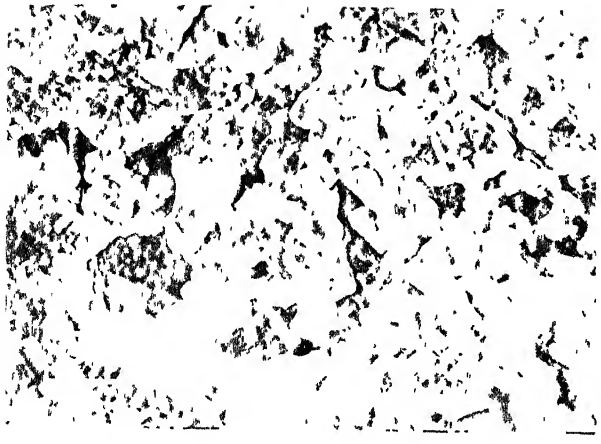

5% TiN

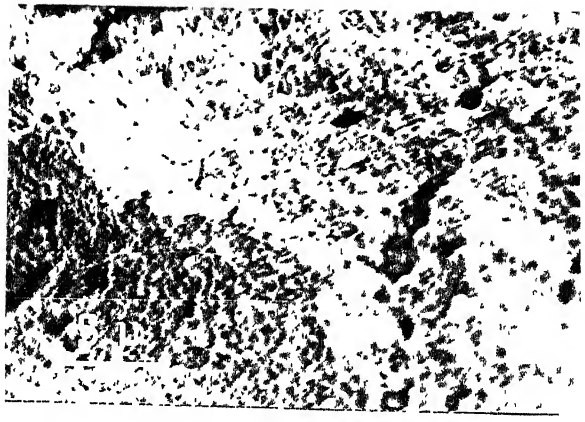

10% TiN

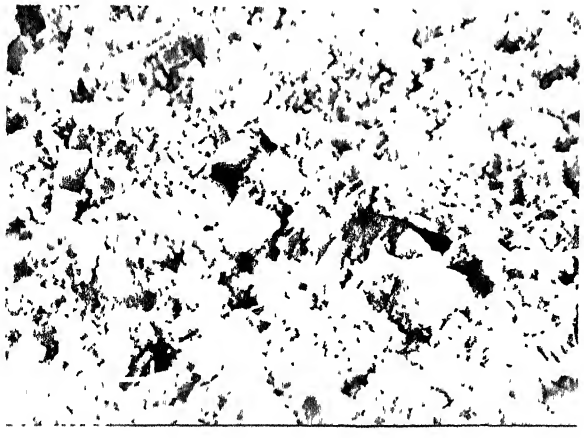

10% TiB_2

Fig. 3.16 Some typical scanning electron fractographs of WC-10 Co hardmetals with refractory compounds addition, sintered at 1400°C for 1 hr in dry H_2.

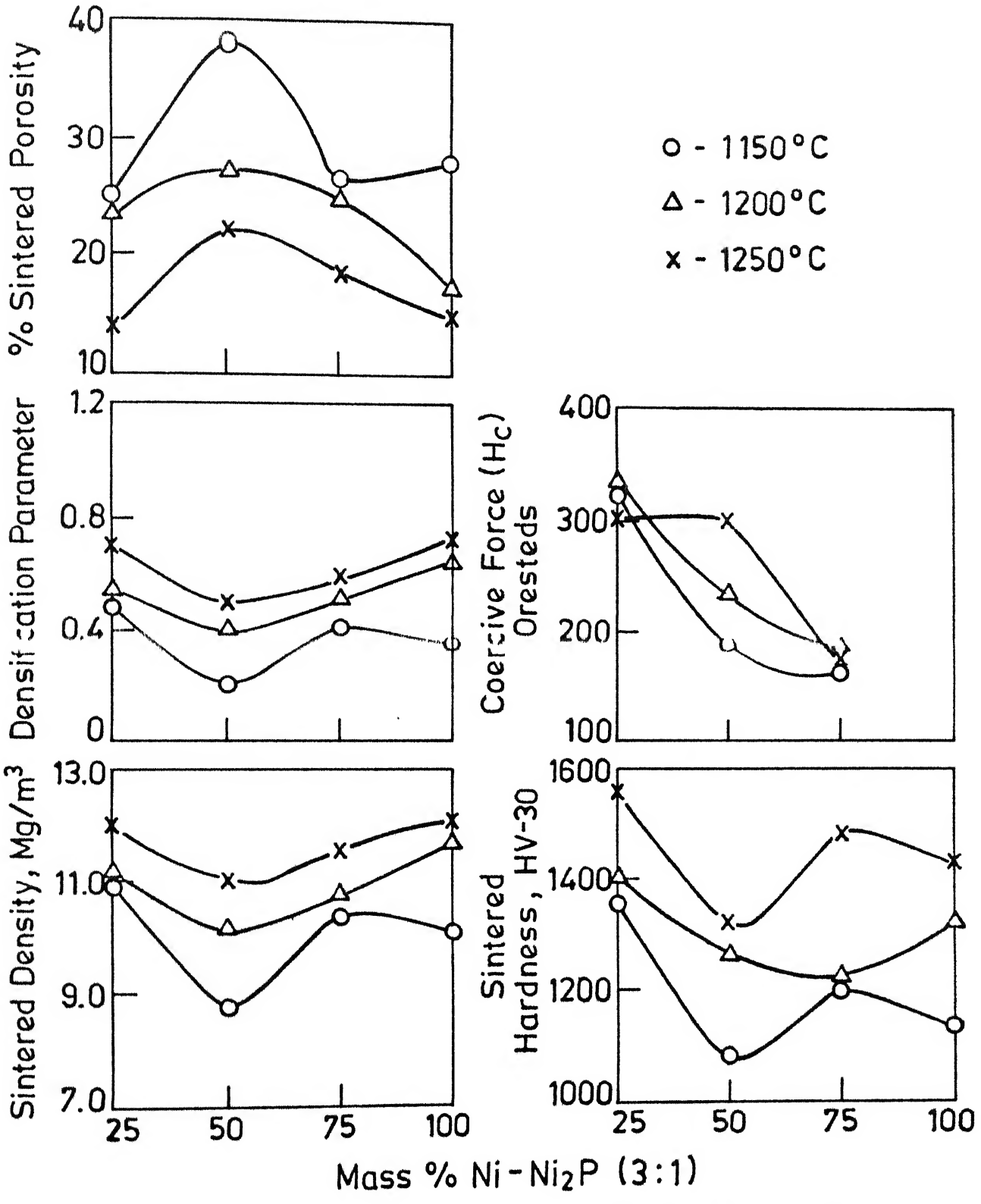

Fig. 3.17 Sintered properties of WC-10%(Co-Ni/Ni P) hard-metals sintered at 1150°C, 1200°C, and 1250°C respectively for 1hr in dry H_2

PART I

IV.2 WC-10 Co/Ni HARDMETALS:

From the experimental results it is evident that partial or complete substitution of Co by Ni gives sintered properties inferior to Co bonded ones which is in agreement with Tracy and Hall.[2] From Figure 3.1 and Figure 3.5 it is seen that with increase in Ni content in the binder both sintered density and hardness decrease with the exception of 50 Co/50 Ni binder hardmetal sintered at 1350°C. An increase in sintering temperature from 1350°C to 1400°C showed better sintered properties, but obviously inferior to the straight cobalt bonded hard metal.

It is well known that WC has excellent wettability with Fe-group transition metals which has been explained elsewhere[52] on the basis of chemical bondings. The solubility of carbide phase into the binder melt can also be explained on the above basis. As the d-configuration of Ni is more or less full, it is natural that WC and Ni compacts would not achieve the maximum possibility of interaction.

Among all the WC-10(Co/Ni) hardmetals investigated, 50 Co/50 Ni hardmetal showed best properties. However, the hardness value of 25 Co/75 Ni binder hardmetal is comparable with that of 50 Co/50 Ni hardmetal, even though a poor densification occurred for this composition. This may be due to the presence of metastable fcc (β) phase of Co retained at room temperature which is liable to deformation induced $\beta - \varepsilon$ transformation giving rise to workhardening effect.[53]

The decrease in T.R.S. values with the addition of Ni to the WC-10 Co hardmetal may be due to the fact that Ni addition promotes free graphite formation in the WC-10(Co/Ni) hardmetal. This occurrence of free graphite gives rise to soft spots and hence an early failure of the specimens.

The decrease in magnetic properties with increase in Ni content in the binder is followed by zero magnetic saturation in case of complete Ni substitution (Figure 3.6). This is in confirmation with the findings of Schwarzkopf and Kieffer[3] and Brabyn et.al.[54] According to the former[3] the introduction of Ni to WC leads to free carbon in the system, while according to the latter,[54] even slightly decarburized WC-Ni hardmetals can show zero magnetic saturation and coercive force.

The increase in grain size after sintering with increase in Ni content in the binder confirms the findings of Rautellea and Norton.[49]

The increase in sintering temperatures from 1350°C to 1400°C shows an improvement in the properties (Figures 3.1 to 3.5). This is a natural consequence of enhanced liquid flow at elevated temperature resulting in better composite sinterability. As far as straight Ni binder is concerned, at 1350°C liquid phase sintering is not operative as the eutectic temperature is still higher i.e. 1380°C. However, at 1400°C, there is no such limitation.

IV.3 WC-10(Co/Fe) HARDMETALS:

It is evident from the results (Figures 3.1 and 3.5) that either partial or complete substitution of Co by Fe in WC-10 Co hardmetal adversely effects their sintered properties. Densification of the hardmetals is better in Fe-rich composition, which is obviously because of the relatively low eutectic temperature of WC-Fe system (1143°C). Though there is no marked change in hardness value with the addition of Fe to WC-10 Co hardmetals but T.R.S. falls drastically with a slight improvement for 100% Fe in the binder. It has been reported[49] that the solubility of WC in Fe is less than that of Co. Wettability of WC by Fe melt is also much inferior to that of Co.

The WC-binder bonding is, therefore, very poor when Co is substituted by Fe in WC-10 Co hardmetal resulting into poor end properties. Another reason may be the presence of η phase with Fe addition.[50]

It is also seen from the results that the sintered properties of the hardmetals are improved with increase in sintering temperature. This is because at higher temperature flowability of the liquid phase formed during sintering and the associated solution-reprecipitation phenomenon resulting into better composite bonding and better homogenization.

IV.4 WC-10(Ni/Fe) HARDMETALS:

It is evident from the results that complete substitution of Co by Ni/Fe in WC-10 Co hardmetal shows better

sintered properties compared to either Ni or Fe substitution (Figures 3.1 and 3.5). Introduction of Ni and Fe in WC-10 Co hardmetal results in free carbon and large grains of 'eta' phase.[3] However, when Ni/Fe binder is used, iron would help in lowering the adverse effect of nickel, thus resulting into improved properties.[50] In the present hardmetal system, 25 Ni/75 Fe binder shows best densification, whereas 50 Ni/ 50 Fe binder hardmetal shows best mechanical properties in spite of their poor densification. This may be due to the fact that 50 Ni/50 Fe hardmetal is free of both graphite and 'eta' phase while 25 Ni/75 Fe hardmetal contains either of the phases stated though better densification is taking place in the latter one.[50] The lower solubility of WC in Fe (7.5%) as compared to that of Ni (15%) should promote carbide coarsening, although this feature is not so prominent in the present findings (Figure 3.6).

IV.5 OXIDATION BEHAVIOUR:

From the oxidation data (Figures 3.11 to 3.12) of the WC-10(Co/Ni) system investigated presently, Figure 4.1 has been plotted to highlight the effect of binder composition on oxidation at 800°C for three periods which are 120, 300 and 480 minutes. Result shows that the weight gain is less pronounced for Co-rich binder (upto 25% Ni) as compared to the Ni-rich binder i.e. (upto 25% Co). In the intermediate range of binder compositions the effect is not so pronounced except in case of 480 minutes oxidation. The X-ray investigations

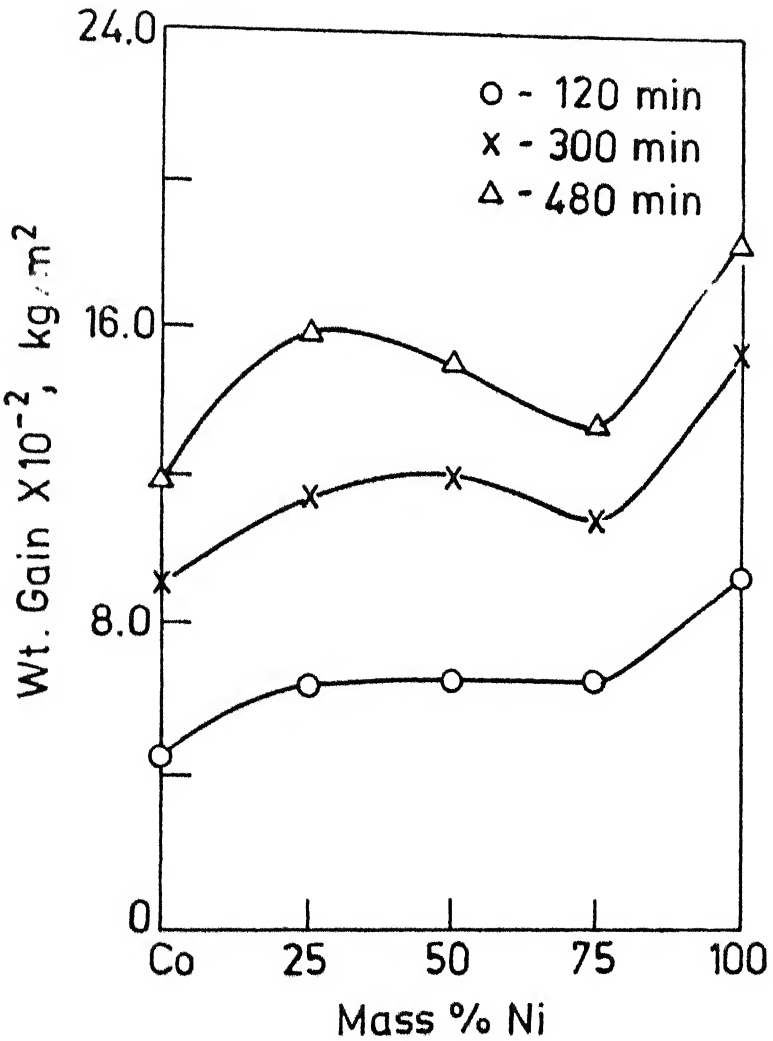

Fig. 4.1 Weight gain vs binder composition of air oxidised WC-10(Co/Ni) hard metal specimens at 800°C for different periods.

carried out also indicate that in concentrated alloy binders the presence of the respective binder metal oxides could not be detected (Appendix I).

The sintered porosity variation in such hardmetal system reveals that porosity increases with increase in Ni in Co-binder, while reverse is true when Co is added to Ni binder. The present oxidation result runs parallel to the porosity variation plot. One thing emerges clearly that out of all the binder compositions straight Co offers maximum oxidation resistance. Cobalt like carbon forms three oxide, cobaltus oxide (CoO), cobaltic oxide (Co_2O_3) and cobalto cobaltic oxide (Co_3O_4). On the other hand Ni forms NiO, Ni_2O and Ni_2O_3. From the thermodynamic data it is noted that change in free energy of formation of oxide at 1100°K for CoO Co_3O_4 are -38,100 cal/gm mole, and -124,650 cal/gm mole respectively whereas the corresponding value for NiO is -33,600 cal/gm mole. These data definitely confirm that the hardmetals containing only cobalt binder is comparatively more oxidation resistant. The stabilization of oxidation response in case of concentrated Co/Ni binary binder may be attributed to the oxidation resistance caused by the solute oxide.

PART II

IV.6 WC-10 Co HARDMETALS WITH REFRACTORY COMPOUNDS ADDITION:

The effects of refractory compounds additions on the properties of WC-10 Co hardmetals are reported in Figures 3.13

) 3.16, from which it is evident that such additions in
neral lower the properties of WC-10 Co hardmetal.

It is well known that WC which is a VIth group metal
rbide, has excellent wettability with Fe group transition
tals, as compared to IVth and Vth group transition metal
rbides. This has been explained elsewhere[52] on the basis
chemical bondings in the respective refractory carbides.
is may be the reason why poor densification occurs with the
dition of TiC or TiC-Mo_2C. However, TiC-Mo_2C addition
ows better properties than TiC. This, in other words, means
at the addition of VIth group metal carbide viz. Mo_2C in
C improves the wettability thus resulting in better proper-
es (Figure 3.13). These carbide additions in WC-10 Co
dmetal decrease hardness, although the individual carbide
s high intrinsic hardness as compared to WC. T.R.S. value
so decreases similar to the hardness variation. However,
er more than 5% addition of TiC or TiC-Mo_2C, the fall in
mechanical properties is a drastic one. This could be
laimed on the basis of the poor wettability, grain coar-
ing response and the higher sintered porosity.

TiN and TiB_2 additives decrease the properties of
10 Co hardmetal respectively. This is because of grain
rsening resulting after such additions due to relatively
r wettability with cobalt. Among these two compounds TiN
ition shows better results and this is obvious, because
is more metallic in nature than TiB_2, thus indicating a
atively better composite bonding in case of the former.
rt from this TiB_2 is more brittle than TiN.

PART III

IV.7 WC-10 Co HARDMETALS CONTAINING Ni/Ni_2P:

The results of the effect of Ni_2P addition in WC-10 (Co/Ni) hardmetal (Figure 3.17) reveal a drastic increase in the sintered porosity values (10 to 40%) in contrast to the hardmetals without any Ni_2P, where the porosity was in upto 12%. Such an effect naturally deteriorates other properties, so much so that T.R.S. measurements could not be made because of their extreme brittleness. However, one similarity in the present case is visible with those samples without any Ni_2P, that the properties variation plots are quantitatively similar with the exception of coercivity, which showed relatively high values.

From Ni-Ni_2P binder phase diagram it has been observed that eutectic forms at 880°C, much below the sintering temperatures selected for the present series of hardmetals. Ito et.al.[56] have confirmed the positive role of Ni_2P addition in sintering of W-Ni system, although this finding does not appear holding true in case of WC-Ni system. A still further intensive study is desirable to fully realise the significance of P.

The positive role of phosphorous addition WC-Co hardmetal in effectively lowering the sintering temperature as reported by Tendolkar,[57] for which an optimum level of 0.35% phosphorous in 91 WC-9 Co hardmetal was established. An increase in the phosphorous level to 0.71% adversely

effected the T.R.S. values, although the amount of liquid phase available during sintering was relatively large. Author attributes this to the slow dissolution of WC in Co_2P containing binder melt and the emergence of brittle Co_2P phase during solidification. Such a finding may also be true in the present investigation as the phosphide content was high upto 2.5% (0.52% P).

CHAPTER V

CONCLUSIONS

(1) The sintered as well as mechanical properties of the WC-10 Co hardmetals decrease with increase in Ni content in the binder. However, 50 Co/50 Ni hardmetal shows the best properties in this series of hardmetals.

(2) Grain size of the carbide phase increases with increase in the Ni content in the binder.

(3) Magnetic properties of the WC-10(Co/Ni) hardmetals fall drastically with increase in Ni content in the binder and ultimately becomes zero, when binder phase contains 100% Ni.

(4) Oxidation resistance of WC-10 Co hardmetals decreases on substitution of Co by Ni in binder.

(5) When Co is substituted by Fe in WC-10 Co hardmetal though their hardness remains almost similar, the T.R.S. values are adversely affected, the worst affected being 25 Co/75 Fe binder hardmetal.

(6) In WC-10(Ni/Fe) hardmetals best mechanical properties were obtained for 50 Ni/50 Fe binder hardmetal, although 25 Ni/75 Fe binder hardmetal showed the best densification.

(7) Complete Co substitution in WC-10 Co hardmetal by Ni/Fe binder gives better properties than the Co substitution by Fe or Ni individual.

(8) Overall properties of the hardmetals improve with increase in the sintering temperature (from 1350°C to 1400°C). This is obvious because at higher temperature flowability of the liquid phase formed during sintering and the associated solution-reprecipitation phenomenon resulting in better composite bonding.

(9) Different refractory compounds like TiC, TiC-Mo_2C, TiN and TiB_2 additions in WC-10 Co hardmetal deteriorate the properties, the worst being TiB_2.

(10) Sintered properties except coercive force fall drastically with the addition of Ni_2P in WC-10(Co/Ni) hardmetals.

REFERENCES

1. K. Voigt, U. Voigt, Neue Hutte 19 (1974) 103.
2. V.A. Tracy and N.R.V. Hall, Conference on Recent Advances in Hardmetal Production, Loughborough, 17-19th Sept. (1979), MPR Pub-Co., U.K.
3. P. Schwarzkopf, R. Kieffer, Cemented Carbides, MacMillan, New York (1960), p. 188.
4. J.L. Ellis, British Patent No. 908,412.
5. C. Agte, Neue Hutte 2 (1957) 537.
6. H. Suzuki, T. Yamamoto, O. Kawakatsu, Jap. Soc. Powder and Powder Met., 14 (1967) 86.
7. H. Suzuki, T. Yamamoto, O. Kawakatsu, Jap. Soc. Powder and Powder Met., 14 (1967) 308.
8. D. Moskowitz, M.J. Ford, M. Humenik, Int. Powder Met., 6 (1970) 55.
9. D. Mosokowitz, In "Modern Developments in Powder Met.", Vol. 10, MPIF, Princeton, 1977, p. 453.
10. A. Hara, S. Yazu, Mech. Behaviour of Metals, 5 (1972) 242.
11. J.E. Mahaffy, W.O. Woods, General Thomas J. Rodman Lab., Water Town, Aarsenal, Rep. Nr. 43/1 (1959).
12. P. Schwarzkopf, R. Kieffer, Cemented Carbides, MacMillan, New York (1960), p. 320.
13. H.E. Exner, Private communication.
14. J. Gurland, J. of Metals, 1954, pp. 285-290.
15. H. Suzuki, H. Kubota, Planseeber Pulvermetallurgy, 14, 1966, pp. 96-109.
16. A. Nishiyama, R. Ishida, Trans. Jap. Inst. Metals., 3, 1962, pp. 185-190.
17. H. Jinmuber and O. Rudiger, Cobalt-19, June, 1963, p. 1.
18. Lardner, Powder Metallurgy, Vol. 13, No. 26, 1970, p. 395.
19. H.E. Exner and H. Fischmeister, Arch, Eisenhuttenwesen, 37, 1966, p. 499.

20. Kenneth J.A. Brookes, World Directory and Handbook of Hardmetals, Int. Carbide Data, U.K.

21. N. Ingeistrom and H. Nordberg, Engineering Fracture Mechanics, Vol. 6 (1974), p. 597.

22. H. Suzuki and K. Hayashi, Planseeber, Pulvermetall, 23 (1975) p. 121.

23. S.B. Luckx, Acta Metall., 23, 1975, p. 109.

24. E.A. Almond and B. Roebuck, Met. Sci., 11, 1979, p. 458.

25. E.W. Engle, Powder Metallurgy (J. Wulff, ed.), Am. Soc. Metal, Ohio, 1942, p. 436.

26. J. Gurland, J. of Metals, Vol. 6(2), (1954) p. 285.

27. E. Lardner, Powder Metallurgy, No. 2 (1978), p. 65.

28. O. Rudiger and H.E. Exner, Powder Metallurgy International, Vol. 8, No. 1 (1976), p. 7.

29. V.I. Tumanov, V.F. Funke, Z.I. Pavlova, T.A. Novikova and K.A. Bystrova, Fiz. Metal. i Metalloved, 15(2), (1963) p. 235.

30. G.S. Kreimer, V.I. Tumanov, D.S. Kamenskaya and Z.I. Pavlova, Fiz. Metal. i Metalloved, 17(4), (1964), p. 572.

31. V.I. Tretjakov, Sintered Hardalloys, Metallurgizdet, Moscow, 1962.

32. R. Warren and H. Hatzke, R 398/81, Presented at the International Conference on Hardmaterials, Wyoming, U.S.A., August, 1981.

33. M. Nakamura and J. Gurland, Metallurgical Transaction, A, Vol. 11A, January (1980), p. 141.

34. J. Gurland and P. Bardzil, J. Metals, Vol. 7 (1955), p. 311.

35. A.B. Platov, Hardalloys, Sb. Tr. Vses Nauchn. Issled. Inst. Tverd. splav., Vol. 2, Metallurgizdt (1960), p. 82.

36. H.C. Lee and J. Gurland, Material Science and Engg., Vol. 33 (1978), p. 125.

37. G. Altmayer and O. Yung, Z. Metallik, Vol. 52(9), (1961), p. 576.

38. H.S. Kalish and N.R. Giblos, Aqans. Carbide Corporation, Kenilworth, New Jersey, June 27-July 2 (1976).

39. M.M. Khmschchov and M.A. Babichev, Vestu. Mashinostar, No. 9 (1954), p. 3.

40. H.S. Shan and P.C. Pandey, 'Wear', 37 (1976), p. 69.

41. B. Roebuck and E.A. Almond, Reprint of Conference on 'Recent Advances in Hardmetal Production', Loughborough, 17-19 Sept., MPR Publicatiens, (1979), p. 28.

42. J. Freytag and H.E. Exner, Proceedings of the 1976 International Powder Metallurgy Conference, Chicago, MPIF, Princeton.

43. W. Dawihl, Handbook of Hardmetals, H.M. Stat. Office, London, (1955), p. 68.

44. R. Edwards, T. Raine, Proc. First Plansee Seminar (1953), p. 232.

45. S. Takeda, Sci. Repts. Tohoku Imp. Univ., Honda Anniv. Issue (1936), p. 864.

46. I.N. Chaporova et.al., Hardmetals Production Technology and Research in U.S.S.R., ed. by S.I. Bashkirov (1964), p. 172.

47. K. Whitehead, L.D. Brownlee, Metrovicks, Elec. Co. Ltd., Research Report No. 5006 (1954).

48. G. Barlow, Proceedings of the 4th Europian Powder Metallurgy symposium, Grenoble, May 1975.

49. P. Rautellea and T. Norton, J. of Metal, Vol. 4 (1952), p. 1045.

50. D. Moskowitz, M.J. Ford and M. Humenik, Jr., International J. of Powder Metallurgy, Vol. 6(4), 1970, p. 55.

51. D. Moskowitz, Proceedings of the 1976 International Powder Metallurgy Conference, Chicago, MPIF, Princeton.

52. G.S. Upadhyaya, In 'Powder Metallurgy Alloy' (Ed. P. Ramkrishnan), Oxford and IBH Publishing Co., New Delhi, 1982, p. 77.

53. D. Basu and G.S. Upadhyaya, Trans. PMAI, Vol. 11 (1984), p. 1.

54. S.M. Brabyn, R. Cooper and C.T. Peters, Proceedings of 10th Plansee seminar (H.M. Ortner, ed.), Vol. 2, Mettelwerke, Plansee, Reutte (1983), p. 675.

55. D. Basu, 'Sintering of Tungsten Carbide Based Hardmetals and Their Properties', M.Tech. Thesis, I.I.T. Kanpur, 1984.

56. H. Ito, Y. Mitashu and S. Tangusuka, J. Jap. Inst. Met., 35 (1971), p. 6.

57. G.S. Tendolker, In 'Powder Metallurgy Alloys', (Ed. P. Ramkrishnan), Oxford and IBH Publishing Co., New Delhi, 1982, pp. 12-21.

APPENDIX I

X-RAY RESULTS

Hardmetals	Peak angle θ (Degree)	d-spacing (Å)	Relative intensity (I/I_o)	Phase identified
WC-10% Co	19.75	2.522	100	
	26.86	1.880	90	WC
	40.64	1.292	80	
	12.92	3.82	100	
	13.68	3.61	100	WO_3
	13.23	3.73	100	
	17.35	2.86	100	
	21.63	2.31	100	Co_2O_3
	28.82	1.76	100	
	17.16	2.89		
	13.30	3.71		$CoWO_4$
	10.66	4.62		
WC-10(Co/Ni)	19.75	2.522	100	
	26.86	1.880	90	WC
	40.64	1.292	80	
	17.16	2.89	100	
	13.30	3.71	30	$CoWO_4$
	10.66	4.62	30	
	17.47	2.84	100	
	20.70	2.41	40	$NiWO_4$
	30.90	1.65	40	
	12.92	3.82	100	
	13.68	3.61	100	WO_3
	13.23	3.73	100	

Contd...

Continued...

WC-10% Ni	19.75	2.522	100	
	26.86	1.880	90	WC
	40.64	1.292	80	
	17.99	2.76	100	
	25.15	2.00	100	Ni_2O_3
	29.00	1.75	100	
	17.47	2.84	100	
	20.70	2.41	40	$NiWO_4$
	30.90	1.65	40	
	12.92	3.82	100	
	13.68	3.61	100	WO_3
	13.23	3.73	100	